Final Progress Report for Research Projects Funded by Health Research Grants

Instructions: Please complete all of the items as instructed. Do not delete instructions. Do not leave any items blank; responses must be provided for all items. If your response to an item is "None", please specify "None" as your response. "Not applicable" is not an acceptable response for any of the items. There is no limit to the length of your response to any question. Responses should be single-spaced, no smaller than 12-point type. The report **must be completed using MS Word**. Submitted reports must be Word documents; they should not be converted to pdf format. Questions? Contact Health Research Program staff at 717-783-2548.

1. **Grantee Institution:** Magee-Womens Research Institute and Foundation

2. **Reporting Period (start and end date of grant award period):** 1/1/13-12/31/13

3. **Grant Contact Person (First Name, M.I., Last Name, Degrees):** Cheryl A. Richards, MBA

4. **Grant Contact Person's Telephone Number:** 412-641-8932

5. **Grant SAP Number:** 4100062212

6. **Project Number and Title of Research Project:** Project 5 - Effects of Telomerase Inhibitors on Centrosomes and Centromeres in Cancer Cells

7. **Start and End Date of Research Project:** 1/1/13-12/31//13

8. **Name of Principal Investigator for the Research Project:** Calvin Simerly, PhD

9. **Research Project Expenses**.

   9(A) Please provide the total amount of health research grant funds spent on this project for the entire duration of the grant, including indirect costs and any interest earned that was spent:

   $ 174,548.98

   9(B) Provide the last names (include first initial if multiple individuals with the same last name are listed) of **all** persons who worked on this research project and were supported with health research funds. Include position titles (Principal Investigator, Graduate Assistant, Post-doctoral Fellow, etc.), percent of effort on project and total health research funds expended for the position. For multiple year projects, if percent of effort varied from year to year, report in the % of Effort column the effort by year 1, 2, 3, etc. of the project (x% Yr 1; z% Yr 2-3).

Last Name, First Name	Position Title	% of Effort on Project	Cost
Calvin Simerly	Research Associate Professor/Principal Investigator	43%	$65,083
Gerald Schatten	Co-Investigator	15%	$39,534

9(C) Provide the names of **all** persons who worked on this research project, but who *were not* supported with health research funds. Include position titles (Research Assistant, Administrative Assistant, etc.) and percent of effort on project. For multiple year projects, if percent of effort varied from year to year, report in the % of Effort column the effort by year 1, 2, 3, etc. of the project (x% Yr 1; z% Yr 2-3).

Last Name, First Name	Position Title	% of Effort on Project
None		

9(D) Provide a list of **all** scientific equipment purchased as part of this research grant, a short description of the value (benefit) derived by the institution from this equipment, and the cost of the equipment.

Type of Scientific Equipment	Value Derived	Cost
None		

10. Co-funding of Research Project during Health Research Grant Award Period. Did this research project receive funding from any other source during the project period when it was supported by the health research grant?

Yes_____ No___x_____

If yes, please indicate the source and amount of other funds:

11. Leveraging of Additional Funds

11(A) As a result of the health research funds provided for this research project, were you able to apply for and/or obtain funding from other sources to continue or expand the research?

Yes_____ No____x_____

If yes, please list the applications submitted (column A), the funding agency (National Institutes of Health—NIH, or other source in column B), the month and year when the application was submitted (column C), and the amount of funds requested (column D). If you have received a notice that the grant will be funded, please indicate the amount of funds to be awarded (column E). If the grant was not funded, insert "not funded" in column E.

Do not include funding from your own institution or from CURE (tobacco settlement funds). Do not include grants submitted prior to the start date of the grant as shown in Question 2. If you list grants submitted within 1-6 months of the start date of this grant, add a statement below the table indicating how the data/results from this project were used to secure that grant.

A. Title of research project on grant application	B. Funding agency (check those that apply)	C. Month and Year Submitted	D. Amount of funds requested:	E. Amount of funds to be awarded:
None	☐NIH ☐ Other federal (specify:_____ _____) ☐ Nonfederal source (specify: _____)		$	$

11(B) Are you planning to apply for additional funding in the future to continue or expand the research?

Yes_____x___ No_____

If yes, please describe your plans: Once these results are verified, we plan to submit an NIH

RO1grant.

12. Future of Research Project. What are the future plans for this research project?

Additional funding from University or private foundation will be sought to verify and solidify our findings in this 1 year pilot study prior to solicitation of a NIH RO1 grant.

13. New Investigator Training and Development. Did students participate in project supported internships or graduate or post-graduate training for at least one semester or one summer?

Yes_____ No___x_____

If yes, how many students? Please specify in the tables below:

	Undergraduate	Masters	Pre-doc	Post-doc
Male				
Female				
Unknown				
Total				

	Undergraduate	Masters	Pre-doc	Post-doc
Hispanic				
Non-Hispanic				
Unknown				
Total				

	Undergraduate	Masters	Pre-doc	Post-doc
White				
Black				
Asian				
Other				
Unknown				
Total				

14. **Recruitment of Out-of–State Researchers**. Did you bring researchers into Pennsylvania to carry out this research project?

    Yes_____ No____x_____

    If yes, please list the name and degree of each researcher and his/her previous affiliation:

15. **Impact on Research Capacity and Quality**. Did the health research project enhance the quality and/or capacity of research at your institution?

    Yes____x_____ No_____

    If yes, describe how improvements in infrastructure, the addition of new investigators, and other resources have led to more and better research.

    This sponsorship was invaluable for the Pennsylvania investigators to develop new sophisticated dynamic approaches for investigating telomerase inhibition in living cancer

cells using a variety of imaged-based and molecular technologies, and will be instrumental in recruiting new National Cancer Institute resources to programs here at the Magee-Womens Research Institute and Foundation. Furthermore, this sponsorship will help to leverage new collaborations to the Commonwealth and we are optimistic that further dividends will accrue.

16. Collaboration, business and community involvement.

16(A) Did the health research funds lead to collaboration with research partners outside of your institution (e.g., entire university, entire hospital system)?

Yes_____ No____x_____

If yes, please describe the collaborations:

16(B) Did the research project result in commercial development of any research products?

Yes_____ No____x_____

If yes, please describe commercial development activities that resulted from the research project:

16(C) Did the research lead to new involvement with the community?

Yes_____ No_____x_____

If yes, please describe involvement with community groups that resulted from the research project:

17. Progress in Achieving Research Goals, Objectives and Aims.

List the project goals, objectives and specific aims (as contained in the grant agreement). Summarize the progress made in achieving these goals, objectives and aims for the period that the project was funded (i.e., from project start date through end date). Indicate whether or not each goal/objective/aim was achieved; if something was not achieved, note the reasons why. Describe the methods used. If changes were made to the research goals/objectives/aims, methods, design or timeline since the original grant application was submitted, please describe the changes. Provide detailed results of the project. Include evidence of the data that was generated and analyzed, and provide tables, graphs, and figures of the data. List published abstracts, poster presentations and scientific meeting presentations at the end of the summary of progress; peer-reviewed publications should be listed under item 20.

This response should be a DETAILED report of the methods and findings. It is not sufficient to state that the work was completed. Insufficient information may result in an unfavorable performance review, which may jeopardize future funding. If research findings are pending publication you must still include enough detail for the expert peer reviewers to evaluate the progress during the course of the project.

Health research grants funded under the Tobacco Settlement Act will be evaluated via a performance review by an expert panel of researchers and clinicians who will assess project work using this Final Progress Report, all project Annual Reports and the project's strategic plan. After the final performance review of each project is complete, approximately 12-16 months after the end of the grant, this Final Progress Report, as well as the Final Performance Review Report containing the comments of the expert review panel, and the grantee's written response to the Final Performance Review Report, will be posted on the CURE Web site.

There is no limit to the length of your response. Responses must be single-spaced below, no smaller than 12-point type. If you cut and paste text from a publication, be sure symbols print properly, e.g., the Greek symbol for alpha (α) and beta (ß) should not print as boxes (□) and include the appropriate citation(s). DO NOT DELETE THESE INSTRUCTIONS.

Goals. Nearly all human cancers bypass replicative senescence and DNA damage signaling pathways by preventing the shortening of telomeres, the protective 'caps' at chromosomal ends, using the reverse transcriptase telomerase. This cancer cell-exclusive enzyme is an ideal biomarker and target for cancer diagnosis, prognosis, and therapies. Genomic instabilities also correlate with centrosomal abnormalities and defects to the spindle assembly checkpoint (SAC) system, increasing spindle multipolarity and chromosome misalignment, a hallmark of many cancers. Here, fixed and dynamic confocal imaging with living markers for centrioles and microtubules are used to explore telomerase inhibitors' impact on centrosome and SAC constituents in normal somatic and cancerous cells.

Objectives and Specific Aims: This research explores whether telomerase inhibitors interfere with centrosome function and duplication or with the protein constituents of the SAC (centromeres) in normal cells and in lung and breast cancer cells. The two specific aims are:

Aim I. What are the effects of Telomerase Inhibitors (TIs) on cancer cell viability, DNA synthesis, metabolic activity, and Telomerase activity?
Question 1. Do TIs impact growth and proliferation of control WI-38 and NCI H292 or MCF7 cancer cells?
Question 2. Do TIs impact DNA synthesis in a dose-dependent manner in control WI-38 and NCI H292 or MCF7 cancer cells?
Question 3. What are the effects of TIs on the metabolic activity of control WI-38 and NCI H292 or MCF7 cancer cells?
Question 4. Do TIs inhibit endogenous telomerase activity in a dose-dependent manner in control WI-38 and NCI H292 or MCF7 cancer cells?

Aim 2. At the maximum effective dose of TI, which inhibits cell growth and proliferation of cancer cells as determined in Aim 1, what are the effects of telomerase inhibition on centrosome and centromere function in control WI-38 and NCI H292 or MCF7 cancer cells?
Question 1. Do TIs impact microtubule (mt) organization from the centrosome and do they affects mt dynamics following drug induced disassembly or rescue from mt depolymerization?
Question 2. Do TIs block centrosome duplication in a dose-dependent manner?
Question 3. Do TIs block cell cycle progression in a dose dependent manner?
Question 4. How do TIs impact proteins involved in centromere assembly and the spindle checkpoint pathway during mitosis*?*

Methods employed include the use of fixed and dynamic confocal microscopic imaging with living markers for centrioles, microtubules, and NuMA on normal and cancer cells after TI exposure to block telomerase activity.

Background and Significance. While the ravages of cancer are a significant health problem for all Americans, improvements in understanding cell cycle regulation and the effects on chromosome alignment during mitosis are leading to pioneering cancer therapies using innovative pharmaceuticals. While promising, traditional cancer interventions still suffer from a high incidence of drug refractoriness, with the breast cancer 10-year recurrence rate at about 20% (1), and 30-75% in lung cancer patients, even after complete surgical resection (2). Cancer stem cells (CSCs) may underlie cancer recurrence, as CSCs drive tumor initiation and growth, indefinitely self-renew, have slow replication compared to differentiated cells populating a tumor, and demonstrate high resistance to chemotherapies and radiotherapy (3,4). Mouse xenotransplantation assays predict many CSCs which share homology with cell surface and nuclear markers of adult and embryonic stem cells. Transplanted CSCs also give rise to all differentiated progeny identified in the original tumor (3), reinforcing their existence. Given their identification, new therapies for cancer treatment must target both the differentiated cells and CSCs for eradicating tumors, reducing relapse and metastasis, and improving overall clinical outcomes for cancer patients.

A hallmark of cancer evolution is the acquisition of indefinite replicative growth. This property is closely tied to telomeres, hexameric DNA repeats localized to chromosome ends that protect against the initiation of DNA damage response elements (5). In normal cells, telomeres shorten with each cell division until replicative senescence, a process that acts as a potent anticancer mechanism (6). Cancer cells bypass replicative senescence by activating one of two telomere maintenance processes: telomerase or alternative lengthening of telomeres (ALT) (7). ALT is rare among cancers (10-15%) and operates by replication of telomeric template DNA through homologous recombination (7). The molecular details of ALT are largely unknown, and no viable anticancer therapies currently exist. For 90% of primary tumors, the ribonucleoprotein telomerase functions to synthesize tandem hexanucleotide repeats of telomeric DNA by reverse transcriptase of human telomerase RNA, or hTERC, and to extend telomere length. This rare genomic alteration initiates unlimited proliferation in cells and contributes indirectly to cancer onset. Although hTERC is ubiquitously expressed in all cells, telomerase activity is robust only in pluripotent stem cells, adult stem/progenitor cells, and cancer cells expressing human telomerase reverse transciptase (hTERT), making this enzyme a good biomarker of CSCs and differentiated cancer cells and a highly selective target for cancer therapy. A number of

telomerase inhibitors (TIs) are currently undergoing clinical trials in conjunction with conventional chemotherapies to produce more robust cancer cell treatment responses and to decrease disease recurrence. Additional evidence confirms that TIs disrupt CSCs, reducing their numbers and proliferation, shortening their telomeres, and inhibiting their ability to form free-floating spherical colonies *in vitro* (5).

Among TIs, BIBR1532 is a non peptidic, non-nucleosidic compound that inhibits the catalytic activity of telomerase (8,9). This compound works in many cancer cells (fibrosacoma, prostate, breast, lung) by blocking the processivity of telomerase enzyme in a dose-dependent manner (IC_{50}= 93nM; 8,10). Other studies relate how BIBR1532 downregulates c-myc and hTERT expression, which induces activation of the Cip and Kip family members of the cyclin-dependent kinase inhibitor p21 and disrupts the Bax/Bcl-2 apoptotic pathway (9). Imetelstat (GRN163L; Geron Corporation), a lipidated N3′-P5′ thio-phosphoramidate 13-mer compound that binds to human telomerase RNA and prevents the formation of active hTERT complexes (rev, 5) in brain, breast, lung, prostate, liver, and stomach cancers, causes telomere shortening, chromosome fusions, anaphase bridges, and apoptosis (11). Currently undergoing Phase II human clinical trials in patients with non-small-cell lung cancer (NSCLC), advanced breast cancer, chronic leukemia, thrombocythemia and myeloma, it is water soluble, cell permeable, acid stable, and nuclease resistant, while forming stable RNA duplexes *in vivo* (5).

Centrosomes, the cell's major microtubule-organizing centers, are comprised of a pair of centrioles surrounded by a protein rich cloud of pericentriolar material that nucleates microtubules and defines their orientation. Centrosomes duplicate once per cell cycle, and their replication fidelity is critical to bipolar spindle assembly and accurate chromosome segregation. In cancers, centrosome hyperamplification is commonly observed, linking tumorigencity and aneuploidy. Higher centrosomal abnormalities strongly correlate to chromosomal instability, multipolar spindles, and eventual malignancy, although some cancer cells cluster supernumerary centrosomes to permit near normal cell division. These rare cells show frequent merotelic kinetochore-microtubule attachments during anaphase, causing low-level chromosome mis-segregation that promotes tumor progression.

Telomere shortening causes replicative senescence when cells fail to protect their chromosomal ends from DNA damage and repair mechanisms. To avoid replicative senescence, ATM and ATR checkpoint pathways must be bypassed in response to DNA double-strand breaks at telomeres that initiates a DNA damage response and p53-mediated cell cycle arrest (5,12). Some cells inactivate p53 and p16/Rb cell cycle checkpoints, extending their division cycles even while losing telomere length. When these cells reach the crisis stage marked by increased genomic instability through chromosome end fusion and aneuploidy, most undergo p53-independent programmed cell death; a minority, however, escapes this fate by activating telomerase and continuing to proliferate indefinitely, a hallmark of cancer onset.

The cell cycle checkpoint pathway is a surveillance system that protects against chromosome mis-segregation. Proteins in this pathway include mitotic arrest deficient-like 1 and 2, known as MAD1L1 and MAD2L1 in mammals; budding uninhibited by benzimidizoles 1 and 3, or Bub1 and Bub3; budding uninhibited by benzimidizoles-related 1, or BubR1; and monopolar spindles 1, or Mps1 (13-15). These proteins are recruited to unattached kinetochores in a hierarchical

manner to undergo enzymatic and conformational activation to inhibit the anaphase-promoting complex/cyclosome (APC/C) bound to its mitotic activator, cdc20, or APC/C^{cdc20}. By stabilizing APC/C substrates, securin and cyclin B1, anaphase onset is delayed until all chromosomes are correctly attached to the mitotic metaphase spindle. Thus, these proteins play significant roles in cell cycle control and tumor suppression by acting at the kinetochore region to monitor chromosomes unattached to the mitotic spindles (16). Chromosomal segregation during mitosis is also regulated by serine/threonine kinases.

The Aurora kinases include Aurora A, B, and C (17). Aurora B localizes to kinetochore microtubules and maintains Mad2L1, BubR1, and centromere proteins (CENP)-A/E at kinetochores. Aurora A is crucial for centrosome segregation, recruitment of γ-tubulin, mitotic spindle assembly, Mad2L1 kinetochore dissociation, and mitotic exit. Aurora C, mostly identified with germ cells, is expressed in some tumor lines (18) and shares homology with some Aurora B substrates, especially chromosomal passenger proteins (19). Never-in-mitosis gene a-related kinase 2 (Nek2) is a kinetochore SAC kinase required for MAD2L1 association and centrosome segregation at G2/M (20).

CENPs mediate the function of kinetochores at chromosomes (21). CENP-A, at the inner layer of the trilaminar kinetochore structure, is an essential histone H3 variant important for recruitment of other CENPs, proper kinetochore assembly, and chromosome segregation. CENP-B, also a kinetochore inner layer protein, facilities centromere assembly and is perhaps a biomarker of NSCLC (22). CENP-K is a constitutively centromere-associated network protein at the kinetochore outer layer required for chromosome congression, maintenance of stable chromosome alignment, and correct timing of metaphase-to-anaphase progression (21). CENP-E, a mitotic kinesin-7 family member bound to the outer fibrous corona, actively participates in the capture/stabilization of kinetochore microtubules and chromosome congression at metaphase.

The connection between TIs, centrosome activity and centromere fidelity are largely unknown in cancer cells. This study seeks to improve the health and well-being of Pennsylvanians by exploring mechanisms which induce cancer cell death through specific TIs, investigating their effects on critical centrosome- and centromere-residing proteins important in chromosomal instability. It will help our Commonwealth by leveraging Federal and international research sponsorship, augmenting collaboration among clinical and basic researchers, helping to generate new intellectual property for further commercialization, and promoting high-technology businesses in the region and throughout the Commonwealth while increasing infrastructure and research workforce capacity. It will answer fundamental and translational problems regarding how TIs work on the largely unexplored areas of centrosomes and centromeres, structures vital to chromosomal fidelity in normal and cancer cells.

Results. The Research goals, objectives, aims, methods, design and timeline did not change from the original grant application, and excellent progress was made on a majority of the questions in the two specific aims. Some slight alterations in cell line usage, TI employment, and inclusion of known drugs to inhibit multidrug resistence genes were subsequently employed during the course of this 1-yr investigation as described below.

Three cell lines were utilized for investigating BIBR1532 in cancer and noncancerous cells: MCF7, a breast cancer cell line; NCI H292, a lung carcinoma line; and CCD-Lu8, a control lung fibroblast line. We found the control cell line WI-38, listed as our control cell in the original grant, to be consistently slow and difficult to propagate in the laboratory, hence the acquisition of a robust new control cell line, CCD-Lu8, for our studies. We also attempted to find a control breast fibroblast line for comparison with the MCF7 breast carcinoma line. Two independent human mammary epithelial cell lines from two commercial companies (Primary Normal Human Mammary Epithelial Cell line, ATCC, catalog number PCS-600-010s; HMEC Human Mammary Epithelial cell line, Lonza, catalog number CC-2551) were purchased and attempts by two skilled cell culturists to establish these lines for our investigations were not successful. Although these lines plated initially, they consistently did not expand in culture conditions using the protocols listed by the manufacturer, and hence, these lines were abandoned. The CCD-Lu8 was grown in Minimal Essential Medium (MEM) + 10% fetal bovine serum (FBS), the MCF7 cell lines were grown in MEM + 10% FBS with 0.01 mg/ml insulin (Sigma, St. Louis, MO) while the NCI H292 lung carcinoma cell line was grown in RPMI media (Life Technologies, Grand Island, NY) with 10% FBS. All cell lines were maintained at 37ºC in a 5% CO_2 incubator and passaged weekly. Frozen stocks of early-passage cells were banked and new cell lines established after ~20 passages *in vitro*.

BIBR (2-[[(2*E*)-3-(2-Naphthalenyl)-1-oxo-2-butenyl1-yl]amino]benzoic acid]1532 was chosen as the exclusive TI for this study as it has been well reported in the literature, is commercially available, and can be prepared as stock solutions (10µM) in DMSO kept at -80ºC. Imetelstat (GRN163L) and the mismatched control compound are proprietary drugs from Geron Corporation (Menlo Park, CA). Significant delays in initiating our 1-year project would have been incurred had we requested use of Imetlestat from the company, owing to lengthy paperwork and material transfer agreements needed between our Research Institute, the University of Pittsburgh, and Geron Corporation.

We also included a multidrug resistant (MDR) inhibitor in our studies not originally described in our grant proposal. Since cancer cells can reverse the efficiency of compounds *in vitro*, using selective MDR genes, we decided to test a third generation MDR inhibitor in combination with BIBR1532: tariquidar [N-[2-[[4-[2-(6,7-Dimethoxy-3,4-dihydro-1H-isoquinolin-2-yl)ethyl]phenyl]carbamoyl]-4,5-dimethoxyphenyl]quinoline-3-carboxamide]. Tariquidar is a reliable inhibitor of the ATP-binding cassette transporter in cancers, has been well reported in the literature, and is commercially available. BIBR153 and tariquidar were prepared as stock solutions in DMSO according to manufacturers' protocols and kept at -80ºC until use.

Aim I. What are the effects of Telomerase Inhibitors (TIs) on cancer cell viability, DNA synthesis, metabolic activity, and Telomerase activity?

<u>Question 1. Do TIs impact growth and proliferation of control WI-38 and NCI H292 or MCF7 cancer cells?</u> To investigate the effects of BIBR1532 TI on cell viability, control and cancer cells were seeded onto 6-well culture plates at 1 x 10^5 cells/ml and incubated in BIBR1532 at 0, 25, 75, and 100 µM for up to 10 days (the time at which control cells showed evidence of contact inhibition). BIBR1532 was replenished every 3 days and cell viability assessed using the trypan blue (Fisher Scientific, Pittsburgh, PA) exclusion assay on Days 4, 7, and 10 post inhibitor

addition. We then plotted the percent viability (viable cell counts/total cell count x 100) against various concentrations of BIBR1532 (Fig. 1) for each cell line. Initially, we included the p-glycoprotein inhibitor tariquidar to block MDR genes in cancer cells (Fig. 1, graphs, left column). In these long-term growth experiments (≥ 4 days), we observed that tariquidar significantly impacted the viability of control CCD-Lu8 cells (Fig. 1, left column, top graph), even in the absence of BIBR1532, compared to the viability of CCD-Lu8 cells without tariquidar (Fig. 1, right column, top graph). Conversely, tariquidar was required for NCI H292 cancer cells (Fig. 1, left column, middle graph) with BIBR1532 when compared to viability analysis in cancer cell lines without the MDR inhibitor (Fig. 1, right column, middle graph), suggesting that this cancer cell line is efficient at blocking the uptake of the TI. For MCF7 breast cancer cells, however, BIBR1532 did impact viability, either with or without tariquidar inhibitor (compare Fig. 1, left and right columns, bottom graphs), although the consistency of TI impact on cell viability was more pronounced in the presence of tariquidar. Regardless, 75-100 µM BIBR1532 exposure in NCI H292 and MCF7 cells grown in the presence of tariquidar demonstrated about a 50% reduction in cell viability by Day 7 post TI addition and 60-70% viability reduction by Day 10 (Fig. 1; left column; middle and lower graphs). CCD-Lu8 control cells without tariquidar MDR inhibitor, however, maintained >90% viability even after 100 µM BIBR1532 for 10 days (Fig. 1; right column; upper graph). We conclude that exposure to ≥ 50 µM BIBR1532 effectively impacts growth and proliferation of NCI H292 and MCF7 cancer cells in the presence of tariquidar MDR inhibitor. Control CCD-Lu8 cells did not appear to be affected by BIBR1532, as expected, since these cells should not have telomerase enzyme, but do show viability loss in the presence of tariquidar inhibitor. Based on these studies, we determined that using ≥ 50 µM BIBR1532 (with tariquidar in cancer cells) would be the minimum inhibitor concentration to use for investigating the effects of TI on centrosome and centromere function in cancer cells.

<u>Question 2. Do TIs impact DNA synthesis in a dose-dependent manner in control WI-38 and NCI H292 or MCF7 cancer cells?</u> We also investigated whether the TI BIBR1532 impacted DNA synthesis onset in a dose-dependent manner in control CCD-Lu8 and the cancer cell lines, NCI H292 and MCF7. We plated all cell lines at a density of 50,000 cells on sterile Thermanox 25mm round plastic coverslips and exposed cells (without tariquidar MDR inhibitor) to 0, 25, 50, 75, or 100µM BIBR1532 for 48 hours. During the final 12 hours of incubation, 10µM 5-bromodexoyuridine (BrdU) was added to each culture. Cells were then fixed in 70% ethanol in 50mM glycine buffer (pH 2.5) for 20 min at -20ºC, rehydrated in phosphate-buffered saline (PBS), and immunostained with anti-BrdU antibody as described by the manufacture's protocols (1:10; Roche Applied Sciences, Mannheim, Germany). Cells for each line were scored for the percent of positive BrdU nuclei (indicating DNA synthesis onset) and plotted against untreated cells for each concentration of BIBR1532 (Figures 2 and 3). We investigated the impact of BIBR1532 on DNA synthesis onset by anti-BrdU in the absence of tariquidar MDR inhibitor (Fig. 2). For control CCD-Lu8 cells, a significant impact on cell proliferation and DNA synthesis onset was observed only at 100µM BIBR1532 (Fig. 2; left graph; purple bar with *). This unexpected finding was surprising, given that CCD-Lu8 cells lack telomerase enzyme (Aim 1, Question 4) and effects on DNA synthesis onset must be related to other unidentified, non-specific effects of this compound. For the NCI H292 lung carcinoma line, no significant impact on DNA synthesis onset was found at any concentration of BIBR1532 unless 1µM tariquidar was included (compare Figs. 2 and 3; middle graphs). These results are consistent with our

findings that the NCI H292 cancer cells have very efficient MDR genes that prevent BIBR1532 from effectively entering cells and blocking telomerase activity in the absence of an MDR inhibitor like tariquidar. By contrast, however, MCF7 breast cancer cells demonstrated a remarkable drop in DNA synthesis onset after ≥50 µM BIBR1532 exposure, even in the absence of the tariquidar inhibitor (compare Figs 2 and 3: right graphs). Figure 4 shows representative image panels of anti-BrdU staining at selected concentrations of BIBR1532 in the presence of 1µM tariquidar (except for control CCD-Lu8 cells where tariquidar was omitted). In general, for cancer cell lines, increasing concentrations of BIBR1532 with tariquidar result in a decrease in the percentage of cells observed to undergo DNA synthesis onset, as expressed by positive anti-BrdU-labeled nuclei. Taken broadly, we have observed a correlation between TI effects on DNA synthesis onset and cell cycle arrest at concentrations of BIBR1532 ≥ 50 µM. However; MDR inhibitors may be required to counteract the efficient reversal of TI by some cancer lines.

Question 3. What are the effects of TIs on the metabolic activity of control WI-38 and NCI H292 or MCF7 cancer cells? We investigated BIBR1532 TI effects on the metabolic activity of control versus cancer cell lines with the Vybrant MTT Cell Proliferation Assay Kit (Molecular Probes, Eugene, OR), using the quick protocol. A 12mM MTT (3-(4,5-dimethylthiazol-2,5-diphenyltetrazolium bromide) stock solution was prepared according to the manufacture's protocol, briefly spun, and stored at 4°C until use. Control and cancer cells were plated in 96-well plates at a density of 5,000 cells per well and incubated in 0, 75, or 100µM BIBR1532 for 24 or 72 hrs. Cancer cells, but not the control CCD Lu8 cell line, were co-incubated with 1µM tariquidar MDR inhibitor. At each time point (24 or 72 hrs), 10 µl of the 12mM MTT stock solution was added to each well and incubated at 37ºC for 4 hrs. After MTT labeling, all but 25 µl of the medium in each well was removed, and then 50µl of anhydrous DMSO added per well, with additional mixing. The samples were then incubated at 37°C, in a humidified chamber, for 10 minutes, mechanically mixed by pipetting, and the absorbance read at 540 nm on a plate reader. For each time point, we plotted 75 and 100µM BIBR1532-treated cells against the control (no drug) wells, set to 100% survival. At 24 hrs post-TI treatment (Fig. 5, left graph), a significant drop in cell proliferation was evident in both NCI H292 and MCF7 cancer cell lines compared to CCD-Lu8 cells within 24 hrs of drug application. The slight increase in the NCI H292 cancer line is probably owing to small pipetting errors in performing the quick protocol technique. Interestingly, after 72 hrs of incubation in BIBR1532, the CCD-Lu8 control cells demonstrated a drop in cell viability, especially at 100µM TI exposure. This supports our earlier findings that higher concentrations of BIBR1532 TI for periods ≥ 24hr demonstrates unanticipated off-target effects in the CCD-Lu8 control fibroblast cell line. Collectively, these data support our initial hypothesis that the MTT assay would show a significant metabolic activity drop in cancer cells after TI application, with the greatest percentage of metabolic loss at doses ≥50µM and exposure time greater than 24hrs. However, higher concentrations of TI do suggest unanticipated drug side effects not related to inhibition of telomerase activity since CCD-Lu8 cells lack telomerase activity (see next question).

Question 4. Do TIs inhibit endogenous telomerase activity in a dose-dependent manner in control WI-38 and NCI H292 or MCF7 cancer cells? To gauge whether BIBR1532 was affecting endogenous telomerase enzyme in cancer cells, we investigated telomerase activity using the TRAPeze Telomerase Detection Kit (Millipore, Temecula, CA). NCI H292 cancer cells were treated with 100 µM BIBR1532, and MCF7 cells were treated with 75 µM BIBR1532, both in

the presence of 1 µM tariquidar, for 72 hrs. Untreated cancer cells (controls) were incubated in 1µM tariquidar alone. CCD-Lu8 cells were exposed to 0, 75 and 100 µM BIBR1532 without tariquidar. Both untreated and TI-exposed cells were collected after trypsin, spun down in a centrifuge at 700 x g, washed once in PBS, and spun again. PBS was removed by a micropipette and the pellets frozen at -80ºC until use. At thaw, samples were suspended in 1x CHAPS lysis buffer and incubated on ice for 30 minutes. Samples were spun in a microcentrifuge at 12,000 x g for 20 min at 4ºC and a small aliquot of each cell line used to determine protein concentration, with the concentration adjusted to 100-500 ng/µl. Since telomerase is a heat-sensitive enzyme, a separate aliquot of each treatment was heated to 85ºC to serve as a negative control. All samples were quickly frozen on dry ice and stored at -80ºC until use. Control samples, including the positive telomerase extract control, PCR amplification control, primer-dimer/PCR contamination control, and the telomerase quantitation control template (TSR8), were prepared as described in the manufacturer's instructions. PCR amplification assay was performed as described in the kit instructions, and the PCR products run on 10% non-denaturing PAGE gel in 0.5X TBE buffer with appropriate molecular weight size markers at 150 V for 1.5 hrs. Bands were visualized with SYBR Green dye according to the manufacturer's instructions. Telomerase activity was calculated as the intensity ratio of the 36-bp standard to the ladder bands, with the percentage of inhibition calculated by comparing the telomerase activity of control versus BIBR1532-treated cells. Both cancer cells lines showed significant reduction (~70%) in endogenous telomerase activity as measured by the TRAPeze assay when compared to tariquidar-treated control cancer lines (Fig. 6, graph; left and middle bars). No telomerase enzymatic activity was identified in the control CCD-Lu8 lung fibroblast line (Fig. 6, graph; far right bars). A representative gel run is shown in Figure 6, lower panel. Of importance, this technique was performed multiple times since false-negative results frequently occur. This was particularily evident when samples had excessively high telomerase activity and the 36-bp band was not visible (Fig. 6, lanes 1, 5, 11, 13, 14), perhaps owing to amplification of the TRAP products and 36-bp band being semi-competitive. Only when runs met all conditions for a valid assay (36-bp internal control band only in the CHAPS buffer lane, the telomerase-positive control lane showing both the 36-bp internal control band and ladder products with 6-base increments starting at 50-bp, and heat-treated samples with no ladder and only the 36-bp internal control band visible) could the assay be utilized to analyze our cell extracts. We were successful in two runs as shown in Figure 6 (graph). Collectively, we demonstrated that BIBR1532 TI caused significant reductions in telomerase activity in our tested cancer, but not control, cell lines.

Aim 2. At the maximum effective dose of TIs which inhibits cell growth and proliferation of cancer cells as determined in Aim 1, what are the effects of telomerase inhibition on centrosome and centromere function in control WI-38 and NCI H292 or MCF7 cancer cells?

<u>Question 1.</u> Do TIs impact microtubule (mt) organization from the centrosome and do they affect mt dynamics following drug induced disassembly or rescue from mt depolymerization? We exposed control and cancer cell lines to either 1µM tariquidar or 100µM BIBR1532 with 1µM tariquidar for 48 hrs. Microtubules were then disassembled with 10µM nocodazole for 1 hr at 37ºC and then either fixed in methanol (no recovery) or permitted to recover in normal culture media for 15 min prior to methanol fixation (rescued). Each sample was immunostained for a centriole marker (CEP 135; Millipore), microtubules (YOL 1/34; Millipore), and Hoechst DNA (Sigma). Fixation times, immunostaining, and image capture parameters (focal depth, laser

settings, image box size, and region of interest) were exactly the same for each cell line and all four treatments. A region of interest (ROI) was drawn around each interphase centriole to include microtubules and the same ROI used for each fixed sample. The microtubule pixel intensity within each ROI was determined using Elements software (n=>6) and average intensity analyzed over three independent trials. The average microtubule pixel intensity in the rescued cell lines was compared to the average microtubule pixel intensity of non-recovered cell lines for each treatment and graphed. As shown in Figure 7, TI with tariquidar did not impact microtubule recovery in CCD-Lu8 cells that lack telomerase activity. However, significantly reduced microtubule recovery was observed in both NCI H292 and MCF7 cells after BIBR1532/tariquidar exposure. Tariquidar exposure alone did not impact microtubule recovery in any cell line.

We repeated the experiments above with a microtubule polymerizing agent, epithilone B, to explore whether BIBR1532 TI affected microtubule dynamics during disassembly of microtubules from the centrosome. As shown in Figure 8, the analysis and conclusions were similar to those reported with nocodazole treatment in that epithilone B did not impact microtubule recovery in CCD-Lu8 cells that lack telomerase activity, while significantly reduced microtubule recovery (disassembly) was observed in both NCI H292 and MCF7 cells after BIBR1532/tariquidar exposure. However, a small difference was noted in the NCI H292 line treated with tariquidar alone, where an impact on microtubule disassembly in the presence of the MDR inhibitor was observed.

Collectively, these data suggest that BIBR1532 impacts microtubule regrowth and disassembly from the centrosomes at interphase, following rescue from microtubule disassembly with nocodazole or microtubule recovery after epithilone B, in cancer cells relative to control cells. Since high TI concentrations block cell cycle progression in cancer cells, we could not accurately determine the effects on mitotic events.

<u>Question 2 Do TIs block centrosome duplication in a dose-dependent manner?</u> Since microtubule dynamics appeared to be impacted by TI, we investigated whether BIBR1532 affected centrosome structure and organization using fixed, stained control and cancer cell lines. In some instances, cells lines in which centrioles were tagged with GFP (green fluorescent protein) centrin were utilized as a second marker of centrosomes. All cell lines were seeded at 50,000 cells per 25mm Thermanox coverslip and grown for 6 days *in vitro* in 0, 25, 75, or 100µM BIBR1532, either with or without 1µM tariquidar MDR inhibitor. After fixation in either absolute cold methanol or 2% formaldehyde in warm PBS (for GFP centrin-tagged lines) for 10 min, cells were rehydrated in PBS with 0.25% Triton X-100 detergent. Centrosomes were detected by standard immunocytochemistry methods, using antibodies to pericentrin (anti-rabbit 4448; 1:500; abCam; Cambridge, MA), an important centrosomal scaffolding protein from which microtubules assemble. Microtubules were detected with a rat anti-tubulin antibody (YOL 1/34; 1:200; Millipore), and DNA was detected with Hoechst dye 33342 (Sigma). All slides were sealed in an antifade solution (Vectashield; Vector Labs, Burlingame, CA) prior to imaging using a Nikon A1 four-laser line confocal microscope equipped with Elements acquisition and analysis software. Importantly, care was taken to fix and process all samples on the same day using exactly the same methods, protocols, and staining solutions for each sample so as to standardize the conditions for analysis. Microscopic imaging of specimens was taken at

exactly the same depth of focus (z-setting), box area size, and laser power settings for all four channels to facilitate comparison between control and drug-exposed samples. For each fixed sample, we counted the number of centrosomes detected by the pericentrin antibody (PC 4448), or GFP centrin, in the cytoplasm of interphase cells (~100-300 cells) and plotted the percentage of cells demonstrating normal centrosome numbers (1-2centrosomes) against the concentration of BIBR1532 tested, as well as non-drug-treated control cells for all three cell lines.

As shown in Figure 9 (graphs, top and middle panels), the control lung cells CCD-Lu8 and lung carcinoma cell line NCI H292 expressed high percentages of normal centrosomes in interphase cells (≥95%), regardless of whether tariquidar was present, as detected by PC 4448 staining profiles. Curiously, at high concentrations of TI (≥50µM), GFP centrin detection was nearly ablated in control CCD-Lu8 and NCI H292 cells. Analysis showed that, despite normal centrosome numbers in CCD-Lu8 and NCI H292 cells, the higher the concentration of BIBR1532 compound, the fewer the number of cells observed on coverslips, overall, and a significant reduction in mitotic cells at concentrations above ≥50µM BIBR1532 was noted (our unpublished observations). We did not detect differences in the surface intensity staining of centrosomes labeled with PC 4448 after BIBR1532 treatment in control CCD-Lu8 or NCI- H292 lung carcinoma cells (Fig. 9E and J).

For MCF7 breast cancer cells, which demonstrate a higher sensitivity to BIBR1532 compound regardless of tariquidar presence (see Figs 1-3, Aim 1), a documented decrease in normal centrosome numbers at interphase was observed at 6 days post BIBR1532 culture above 75 µM, although this reduction was not statistically significant when compared to non-drug-treated control cells (Fig. 10A and B, top graphs). As before, fewer overall cell numbers, with vastly reduced mitotic stages, were observed after treatment with 100 µM BIBR1532 (our unpublished observations). In control GFP centrin-tagged MCF7 cells, anti-pericentrin PC4448-stained interphase centrosomes expressing GFP centrin-tagged centrioles (Fig. 10C) and microtubules were visualized radiating from these microtubule-organizing centers. However, some GFP centrin MCF7 cells grown in the presence of 100 µM BIBR1532 for 6 days did show decreased anti-PC 4448 staining and reduced microtubule organization from the microtubule-organizing center (Fig. 10D: lower left cell) compared to adjacent cells (Fig.10D: compare to upper right cell). Curiously, we also observed absent GFP centrin-tagged centrioles in the BIBR1532 samples compared to adjacent non-affected cells (Fig. 10D; inset, green arrows; compare lower to upper cells). We measured centrosome surface intensity profiles after drawing an ROI around selected centrosomes in BIBR1532-exposed cells (Fig. 10E). Software analysis of the surface intensity profiles demonstrated remarkably lower fluorescence of PC 4448 in centrosomes of select TI-treated MCF7 cells (Fig. 10F) although, presently, we cannot show statistical relevance. Collectively, BIBR1532 may impact centrosomal protein mis-expression in pericentrosomal material and, perhaps, in centrioles in MCF7 cancer cells, leading to disruptions in microtubule dynamics during interphase.

We next decided to use stably transduced GFP centrin-tagged MCF7 cell lines to dynamically image centrioles in the absence or presence of BIBR1532 and tariquidar by time-lapse video microscopy (TLVM). GFP centrin-tagged cells were plated onto sterile 35-mm Matek glass bottom petri dishes and imaged on a Nikon Eclipse T_i inverted microscope equipped with Perfect Focus to prevent Z-axis drifting during prolonged live-imaging. A high-resolution objective

(Plan Fluor oil x100 objective [NA=1.3]) was employed to capture images using an Andor charge-coupled device camera and Nikon Elements software. Cells were maintained at 37ºC and 5% CO_2 using a Tokai stage top incubator. Cancer cells exposed to 1µM tariquidar for 48 hrs did not interfere with assembly of a bipolar spindle with centrioles located at each spindle pole (Fig. 11A-D), which ultimately underwent normal cell division (Fig. 11D, inset; n=3). However, simultaneous exposure to 75µM BIBR1532 and 1µM tariquidar for 48 hrs severely slowed cell cycle progression, and rarely were mitotic MCF7 cells observed. In two imaging sessions, MCF7 cells exposed to BIBR1532 and tariquidar were observed to round up, transition into mitosis, and undergo nuclear envelope breakdown. As shown in Figure 11E-H, a single cytoplasmic centriole did not duplicate or separate at mitotic onset. This cell did not complete cell division even after 9 hrs. The exposure of MCF7 cells to TI and tariquidar was reversible after 48 hrs rescue in normal culture medium (Fig. 11I-L). Rescue cells entered mitosis, assembled a bipolar spindle with centrioles at each spindle pole and divided within ~1 hr of TLVM. For GFP centrin-tagged NCI H292 cells, no cells exposed to 75µM BIBR1532 and 1 µM tariquidar entered into mitosis (n=5; data not shown). Taken together, we demonstrated abnormal centriole behavior in live MCF7cancer cells following BIBR1532 treatment. Centrioles did not duplicate, as only a single centriole was observed in the cytoplasm. Mitosis was rarely detected after high-TI exposure and did not proceed normally, displaying abnormal mitotic spindle assembly, mis-segregated centrosomes, and failure to complete cell division.

Question 3. Do TIs block cell cycle progression in a dose dependent manner? This question was to employ the use of a transiently expressed, live fluorescent-tagged G1 cell cycle phase marker probe (pCORON1002-EGFP-C1-PSLD; GE Healthcare, Pittsburgh, PA) to investigate whether cell cycle progression was impaired with increasing concentrations of BIBR1532 TI. Although we did not attempt to use this particular probe in this single-year study, the answer to whether BIBR1532 impacted cell cycle progression in normal and cancer cells was determined in Aim1, Questions 1-3 and Aim 2, Question 2. Briefly, concentrations of BIBR1532 ≥50µM did impact cell proliferation, mitotic onset and cell division. Although we do not yet know precisely where in the cell cycle TI-inhibited cancer cells are arresting, TLVM of GFP centrin-expressing MCF7 cancer cells suggest that centrioles are not duplicating, perhaps indicating that cells are blocked in the G1-S phase. Confirmation of this will have to await future investigations.

Question 4. How do TIs impact proteins involved in centromere assembly and the spindle checkpoint pathway during mitosis*?* We next wanted to explore whether BIBR1532, with or without tariquidar, impacted various proteins involved in centromere assembly and the SAC pathway. As shown above, in the first two questions of this Aim, however, 100µM BIBR1532 in the cancer lines significantly impacted cell cycle progression with few, if any, mitotic cells on treated coverslips. Also, almost all of the proteins tested only express during mitosis. Given these limitations, we did test four proteins involved in regulation of the mitotic metaphase checkpoint assembly and cell division (Table 1). We plated all cell lines at a density of 50,000 cells on sterile Thermanox 25mm round plastic coverslips and exposed cells to either 1µM tariquidar MDR inhibitor or 1µM tariquidar with 100µM BIBR1532 for 48 hrs before fixation in 2% formaldehyde in warm PBS for 15 min. After a PBS rinse, cells were permeabilized in PBS with 0.25% Triton X-100 detergent (PBS-Tx) for 20 min, then blocked in PBS with 150mM glycine and 3mg/ml BSA for 30 min before application of primary antibodies diluted in PBS (1:800). After overnight incubation in primary antibody, cells were rinsed in PBS-Tx for 30 min

and appropriate secondary antibodies, diluted 1:500 in PBS were applied for 2 hrs at room temperature. The penultimate rinse in PBS-Tx included 10µg/ml Hoechst stain to label DNA and coverslips mounted in an antifade solution (Vectashield; Vector Labs) to retard photobleaching. All cells were imaged with the Nikon A-1 laser confocal microscope and were taken at the same laser exposure, capture time, and z-depth for comparison of different treatments.

Aurora A, a member of the serine/threonine kinase family, important for centrosome segregation, recruitment of γ-tubulin, and mitotic spindle assembly, was tested in all three cell lines (Table 1). As shown in Figure 12A-C for the CCD-Lu8 control lung fibroblast cell line, Aurora A detected spindle pole centrosomes during metaphase when exposed either to 1µM tariquidar or to simultaneous treatment with 1µM tariquidar and 100µM BIBR1532 TI. This pattern persisted even during cell division. Conversely, while the lung carcinoma line, NCI H292, demonstrated similar strong Aurora A centrosomal labeling in the control (Fig. 12D) and1µM tariquidar-treated cells (Fig. 12E), Aurora A centrosome detection was significantly reduced at all mitotic stages after simultaneous exposure to 1µM tariquidar and 100µM BIBR1532 for 48 hrs (Fig. 12F-G). Significantly, very few mitotic cells were observed in NCI H292 after BIBR1532 exposure (<10 per coverslip), and rarely were stages after metaphase seen, suggesting that cell death was significant at anaphase transition following TI treatment. Nevertheless, it is interesting that Aurora A, which recruits γ-tubulin, responsible for nucleating centrosomal microtubules, is impacted in BIBR1532 cancer cells and might explain the reduction in microtubule dynamics observed after nocodazole or epithilone B treatment (Aim 2, Question 1).

We also tested an antibody to Aurora B kinase, which is a known regulator of centrosome function, bipolar spindle assembly, and chromosome segregation, in a variety of cancer cells. Aurora B is also known to bind end-binding protein 1, which regulates microtubule dynamics. As shown in Table 1, however, observations of the effects of short term exposure of BIBR1532 on Aurora B localization patterns on chromosomes and centromeres in NCI H292 and MCF7 mitotic cells were inconclusive. We observed weak-to-moderate staining of control and cancer cells regardless of tariquidar or BIBR1532 exposure. Perhaps the TI exposure was too short for us to see an effect on this mitotic kinase. Understanding the role of Aurora B kinase after TI treatment must await future investigations.

Finally, we tested localization patterns for mitotic assembly checkpoint proteins Bub1 (Fig. 13) and Mad1 (Table 1) in control and cancer cells after BIBR1532. The serine/threonine protein kinase Bub1 is known to bind kinetochores and play a key role in chromosome congression. Bub1 is a master regulator of SAC formation and signaling, where it serves an important role to recruit other SAC proteins such as Mad1, Mad2, BubR1, Cenp-E and Plk1 to the kinetochore. In NCI H292 cells, the strongest detection of Bub1 association with kinetochores was in non-drug-treated (control) prophase cells (Fig. 13A; green). Exposure of NCI H292 cells to 1µM tariquidar, or simultaneous exposure to 1µM tariquidar with 100µM BIBR1532, showed a reduction in Bub1 kinetochore detection at prophase/prometaphase (Fig. 13B and C). Typically, the Bub1 staining in these treated cells appeared as diffuse foci throughout the assembling microtubules and aligning chromosomes. Conversely, detection of Bub1 in MCF7 breast cancer cells was weak in control (Fig. 13D) and 1µM tariquidar-exposed cells (Fig. 13E) compared to the moderate Bub1 detection in MCF7 cells treated simultaneously with 1µM tariquidar and

100μM BIBR1532 (Fig. 13F). Mad1L1 is a conserved SAC signaling protein important for monitoring unattached kinetochores to the mitotic spindle and preventing anaphase onset until all chromosomes have achieved proper attachment. Mad1 antibody was difficult to detect in NCI H292 cells regardless of treatment (Table 1). In MCF7 cells treated simultaneously with 1μM tariquidar and 100μM BIBR1532, Mad1 demonstrated inappropriate spindle pole localization compared to reports of Mad1 localization to centromeres during early mitotic stages, spindle midzone during anaphase, and the midbody during telophase (data not shown). Other antibodies to components of the SAC, like CenpE, BubR1, and Mad2, were used in immunocytochemistry studies, in control and cancer cells, after BIBR1532 exposure, but were not detected in our cells with the methods employed.

These early investigations on BIBR1532 effects on SAC proteins and kinases responsible for cell proliferation are tantalizing, if yet incomplete in scope. Mitotic kinases like Aurora A, that recruit centrosomal proteins important for microtubule nucleation (i.e., γ-tubulin), show reduced detection at the mitotic organizing centers and may provide interesting mechanistic pathways for exploring connections between telomerase inhibition and cytoskeletal dynamics not previously appreciated. The dissection of affected SAC components after TI must await future studies, but may promise unique insights in fundamental and translational problems regarding the little-explored area of how TIs work on centrosomes and centromeres, structures vital to chromosomal fidelity in normal and cancer cells.

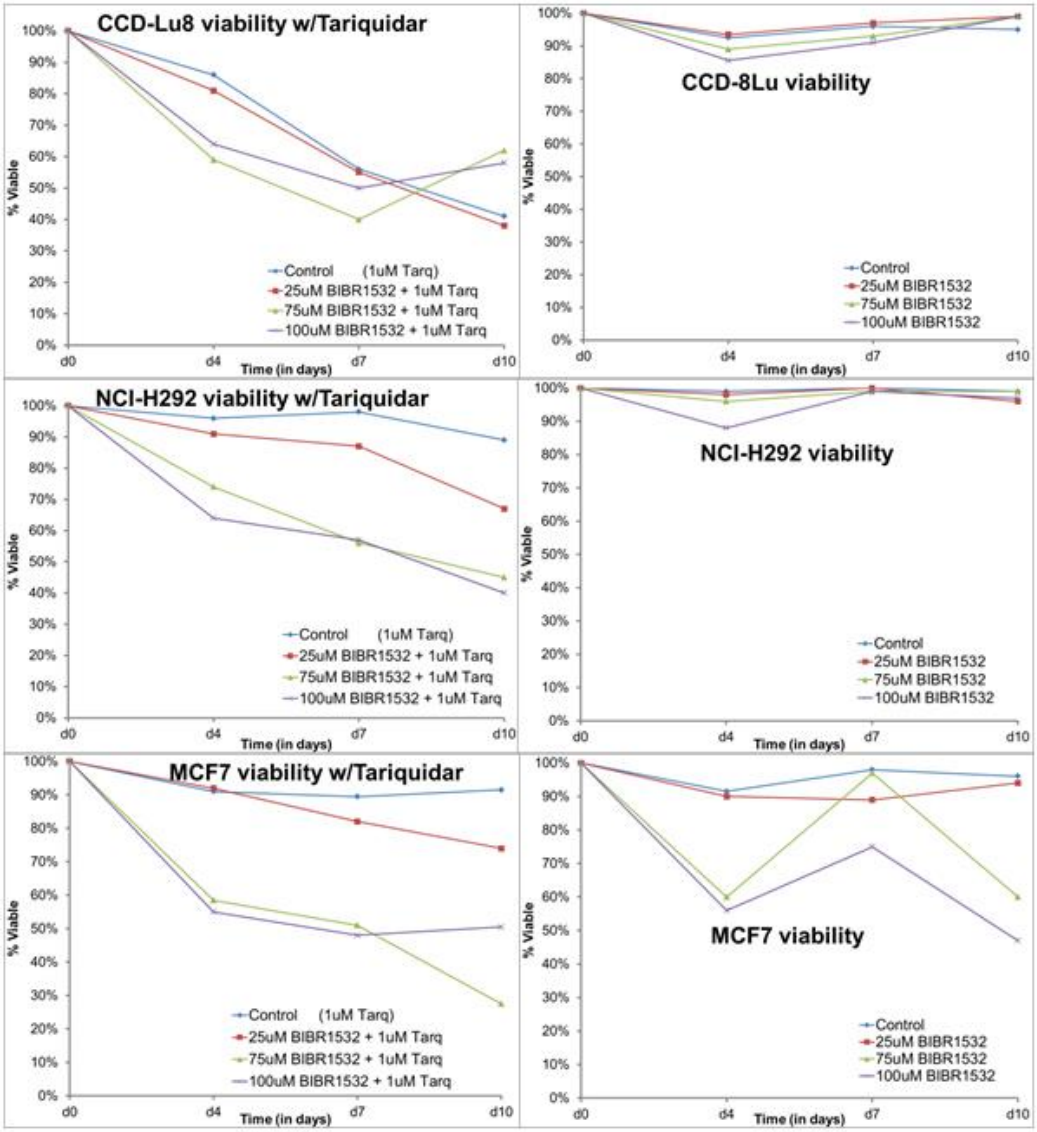

Figure 1. BIBR1532 telomerase inhibitor effects on the viability index of control (CCD-Lu8) and cancer cell lines (NCI H292 and MCF7). Cell lines were treated with 25, 75, or 100μM BIBR1532 with (left column) or without (right column) the multidrug resistance (MDR) compound tariquidar (1μM) and viability assayed using the trypan blue exclusion method at 4, 7, and 10 days post-plating. Analysis suggests that control CCD-Lu8 cells demonstrate reduced viability in the presence of the MDR drug tariquidar (top left graph) while both cancer cell lines require MDR inhibition for effective BIBR1532 telomerase inhibition (left graph, middle and bottom). Percent viability was determined as viable cell counts/total cell count x 100. Values represent two trials.

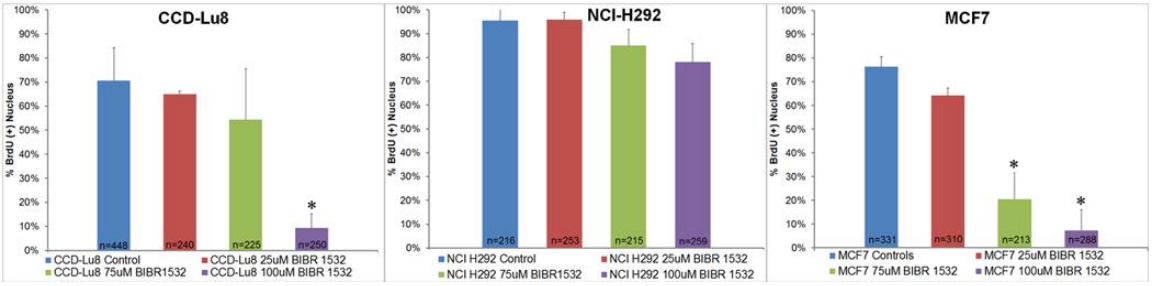

Figure 2. BIBR1532 effects on DNA synthesis in control (CCD-Lu8) and cancer cell lines (NCI H292 and MCF7) without tariquidar MDR inhibitor. Cells from all three lines were seeded independently at 10,000 cells per 25 mm coverslip and treated for 48 hrs in 0, 25 μM, 75 μM, or 100 μM BIBR1532. During the final 12 hrs of telomerase inhibitor exposure, 10 μM BrDU was added to the culture medium prior to fixation and anti-BrdU staining. Coverslips were scored for the percent of positive BrDU nuclei (i.e., DNA synthesis onset) and plotted against untreated cells for each concentration of BIBR1532. Numbers represent total cells counted in ≥ 5 trials. *; significant difference from non-BIBR1532 cells ($p < 0.05$).

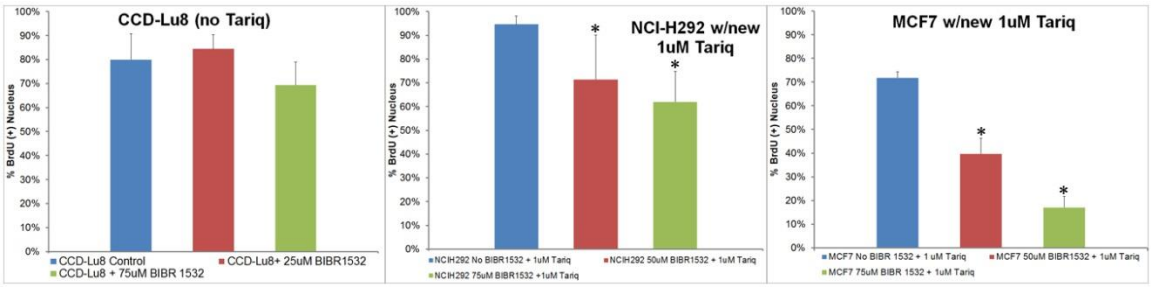

Figure 3. BIBR1532 effects on DNA synthesis in control (CCD-Lu8) and cancer cell lines (NCI H292 and MCF7) with 1μM tariquidar MDR inhibitor in cancer cells. Cells from all three lines were seeded independently at 10,000 cells per 25 mm coverslip and treated for 48 hrs in 0, 25, or 75 μM BIBR1532. During the final 12 hrs of telomerase inhibitor exposure, 10 μM BrDU was added to the culture medium prior to fixation and anti-BrdU staining. Coverslips were scored for the percent of positive BrDU nuclei (i.e., DNA synthesis onset) and plotted against untreated cells for each concentration of BIBR1532. Numbers represent total cells counted in ≥ 5 trials. *; significant difference from non-BIBR1532 cells ($p < 0.05$).

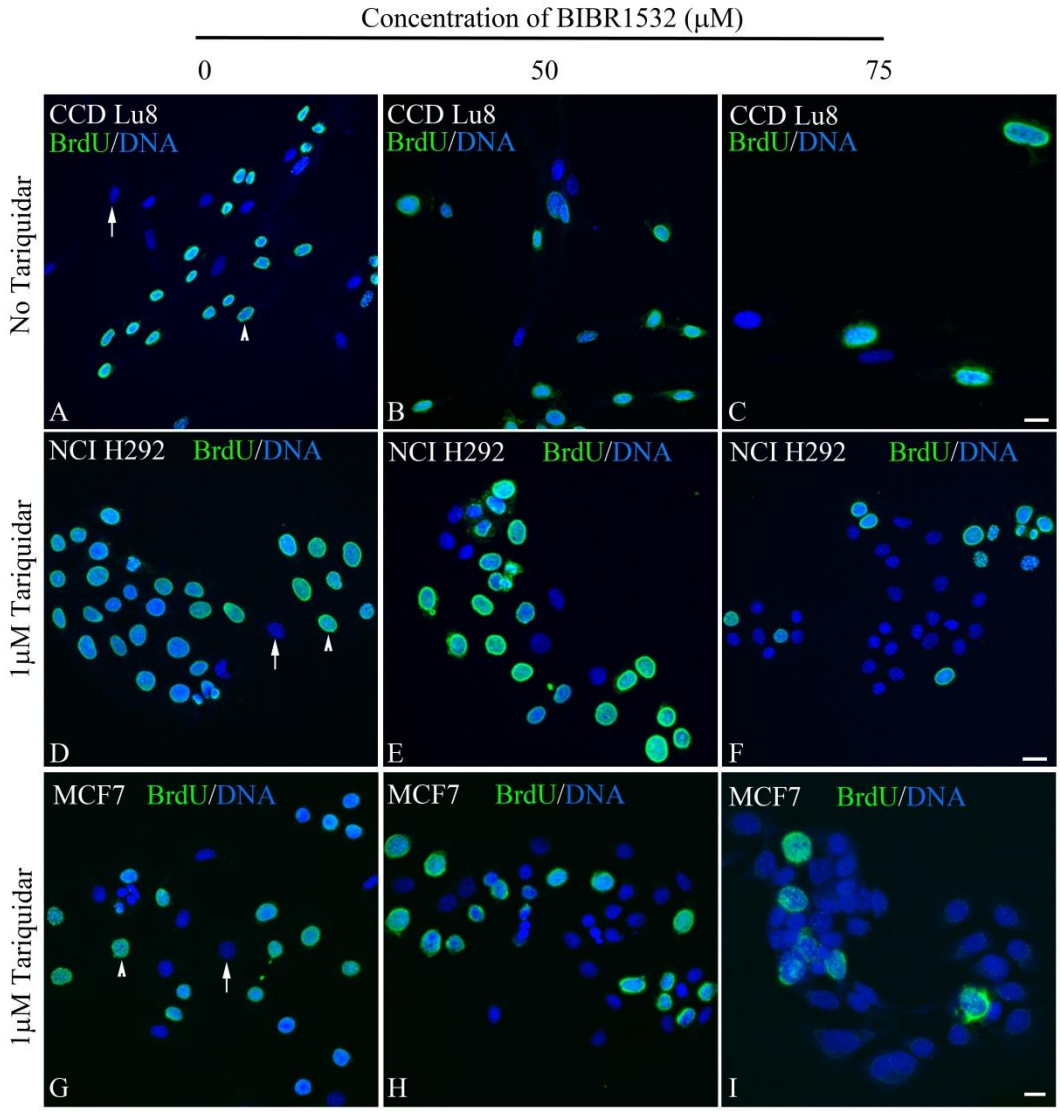

Figure 4. DNA synthesis onset detected with anti-BrdU in CCD-Lu8, NCI H292, and MCF7 cells after BIBR1532 exposure. A-C: control CCD-Lu8 cells without tariquidar, showing percentage of cells lacking detectable nuclear BrdU staining in control, 50, and 75μM BIBR1532 telomerase inhibitor. Although fewer (+) BrdU-labeled nuclei are present in the 75μM BIBR1532, the overall percent decrease in DNA synthesis onset was not significant compared to control cells (see Fig. 3). D-F: NCI H292 lung carcinoma cells demonstrate significant reduction in the detection of (+) BrdU-labeled nuclei with increasing concentration of BIBR1532. G-I: MCF7 breast adenocarcinoma cancer cells showing similar reduction of (+) BrDU nuclei within increasing BIBR1532 concentration, as observed in the lung carcinoma cell line. All images are double- labeled for anti-BrdU (green) and Hoechst DNA (blue). Arrows: nuclei not undergoing DNA synthesis; arrowheads: DNA synthesis onset detected with anti-BrdU (green). Scale bars= 5μm.

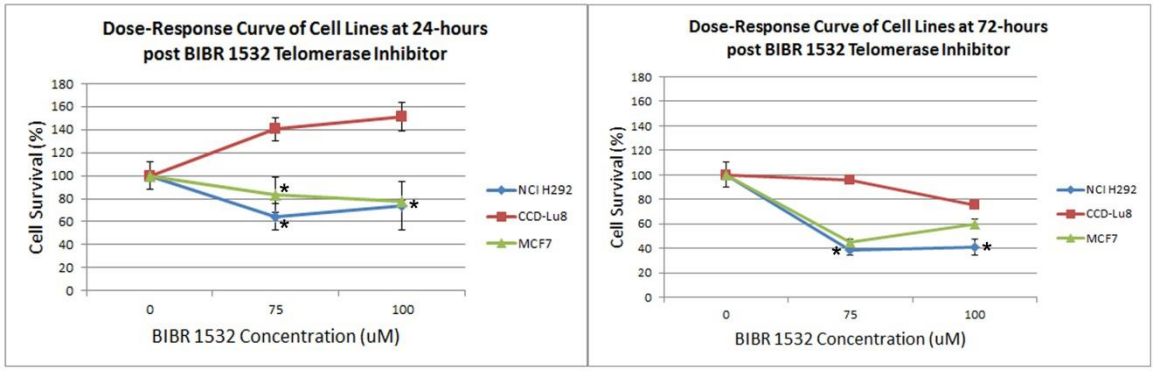

Figure 5. Analysis of BIBR1532 effects on metabolic activity of control and cancer cells as measured by the MTT assay. Control and cancer cells were treated with the designated concentrations of BIBR1532 for 24 or 72 hrs prior to MTT assay analysis. NCI H292 and MCF7, but not CCD-Lu8, were simultaneously treated with 1µM tariquidar. Shown plotted are the percentages of cell survival against the inhibitory effect of BIBR1532 concentrations after 24 or 72 hrs. Values are mean ± SD of three independent experiments. ∗: $p < .05$, significant changes from CCD-Lu8 control cells (red line).

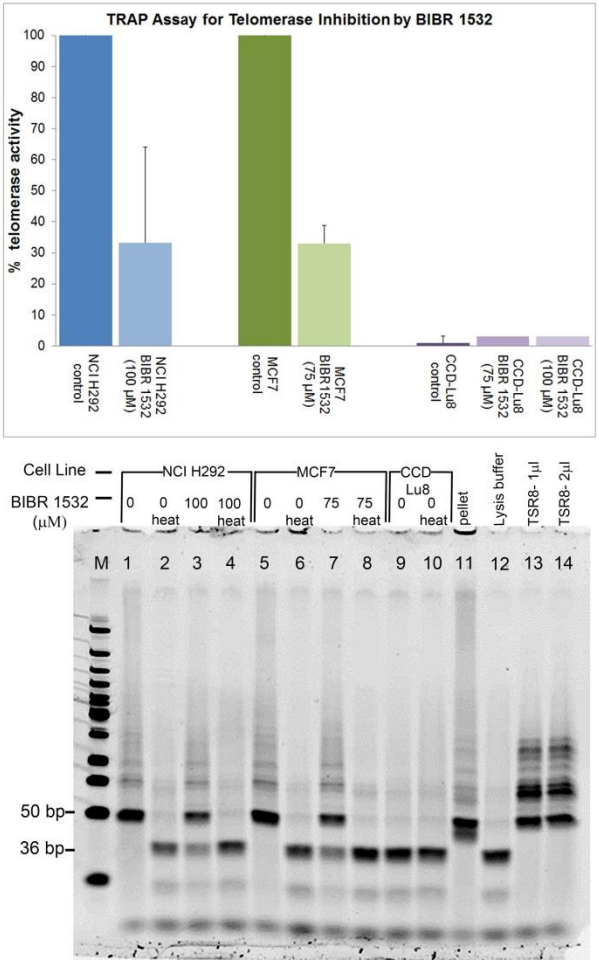

Figure 6. Telomerase enzymatic activity inhibition by BIBR1532 in control and cancer cell lines. NCI H292 cells treated with 100µM, MCF7 cells with 75µM, and CCD-Lu8 with both 75µM and 100µM BIBR1532. 1µM tariquidar was included in cancer cell lines. After 72 hr, telomerase activity (TA) was determined using the PCR-based TRAPeze assay resolved on 10% PAGE with Sybr Green band detection. TA was calculated using the intensity ratio between the 36-bp standard and ladder bands, with the percentage of inhibition calculated by comparing TA of control versus BIBR1532-treated cells. Upper graph: Telomerase activity is significantly reduced in both NCI H292 and MCF7 cancer cells, but not in the control CCD-Lu8 fibroblast line, which lacks telomerase enzyme. Values are given as mean ± standard error of two independent experiments. *: $p<0.05$ significance from control lines. Bottom gel: TRAP PCR 6% PAGE gel showing 36-bp band and telomerase ladder in NCI H292 lung carcinoma (lanes 1-4), MCF7 breast cancer (lanes 5-8), CCD-Lu8 control lung fibroblasts (lanes 9 and 10), and standard controls (lanes 11-14). Here, the 36-bp band is absent in five samples, owing to high telomerase activity (i.e., lanes 1, 5, 11, 13, 14).

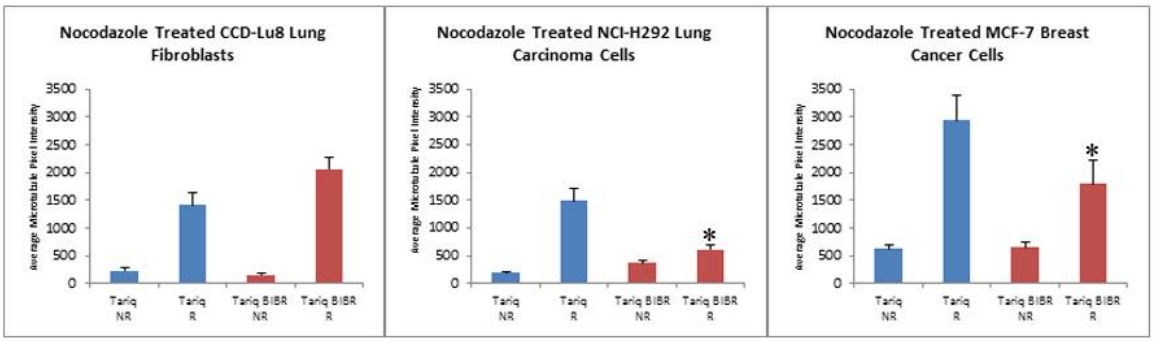

Figure 7. Microtubule recovery dynamics after 10µM nocodazole treatment in CCD-Lu8 control, NCI H292 lung carcinoma, and MCF7 breast cancer cells following exposure to BIBR1532 and tariquidar. Cell lines were treated in either 1µM tariquidar alone (blue bars) or combined 100µM BIBR1532 and 1µM tariquidar (red bars) for 48hrs. After 48 hrs, the microtubule depolymerization agent nocodazole was added to a final concentration of 10µM and incubated for 1 hr in the presence of the telomerase inhibitor and/or MDR inhibitor compounds. Cells were then either fixed in absolute methanol (NR: no rescue) or first permitted a 15-min recovery in normal culture medium (R: rescue) prior to methanol fixation. All samples were stained with antibodies to centrioles and microtubules, along with Hoechst DNA, and then imaged on a Nikon A1 confocal microscope using a Plan Fluor x100 objective (N.A.=1.3) under identical microscope settings, as described (see Aim II, Question 1). In fixed, immunostained interphase cells (≥ 6), a region of interest (ROI) was dawn around the centrioles using Elements image acquisition software. The microtubule pixel intensity was measured within each ROI, averaged for all samples from a particular treatment, and the average microtubule pixel intensity plotted for microtubule recovery (R) versus microtubule disassembly (NR) for each cell line, following either tariquidar or BIBR1532/tariquidar exposure. Average pixel intensity was analyzed by the Student's two-tailed t-test, with p value < 0.05, representing significant difference from the tariquidar control values (*), indicating lower overall microtubule recovery from nocodazole treatment.

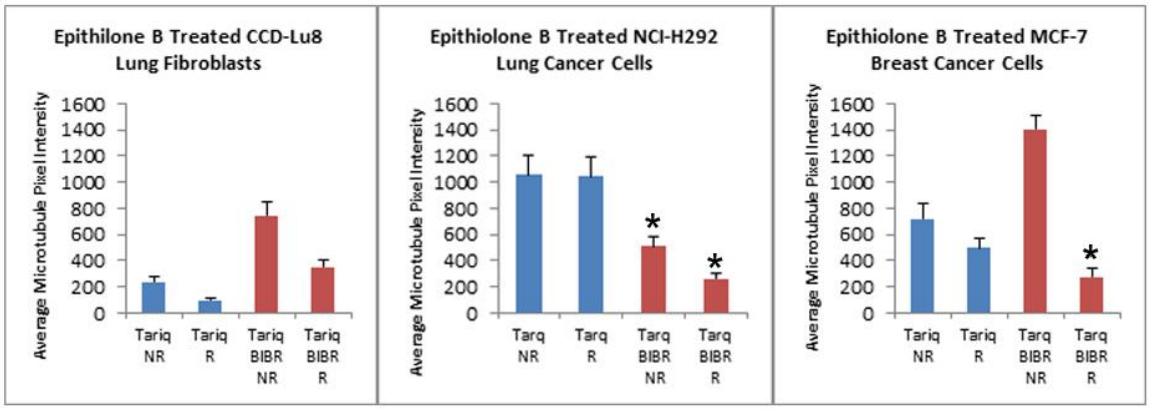

Figure 8. Microtubule recovery dynamics after 10µM epithilone B treatment in CCD-Lu8 control, NCI H292 lung carcinoma, and MCF7 breast cancer cells following exposure to BIBR1532 and tariquidar. Cells were treated in either 1µM tariquidar alone (blue bars) or combined 100µM BIBR1532 and 1µM tariquidar (red bars) for 48 hrs. After 48 hrs, the microtubule polymerizing agent epithilone B was added to a final concentration of 10µM and incubated for 30 min in the presence of the telomerase inhibitor and/or MDR inhibitor compounds. Cells were then either fixed in absolute methanol (NR: no rescue) or first permitted a 15-min recovery in normal culture medium (R: rescue) prior to methanol fixation. All samples were stained with antibodies to centrioles and microtubules, along with Hoechst DNA, and then imaged on a Nikon A1 confocal microscope using a Plan Fluor x100 objective (N.A.=1.3) under identical microscope settings as described (see Aim II, Question 1). In fixed, immunostained interphase cells (≥ 6), a region of interest (ROI) was dawn around the centrioles using Elements image acquisition software. The microtubule pixel intensity was measured within each ROI, averaged for all samples from a particular treatment, and the average microtubule pixel intensity plotted for microtubule recovery (R) versus microtubule disassembly (NR) for each cell line, following either tariquidar or BIBR1532/tariquidar exposure. Average pixel intensity was analyzed by the Student's two-tailed t-test, with p value < 0.05, representing significant difference from the tariquidar control values (*), indicating lower overall microtubule disassembly from epithilone B rescue.

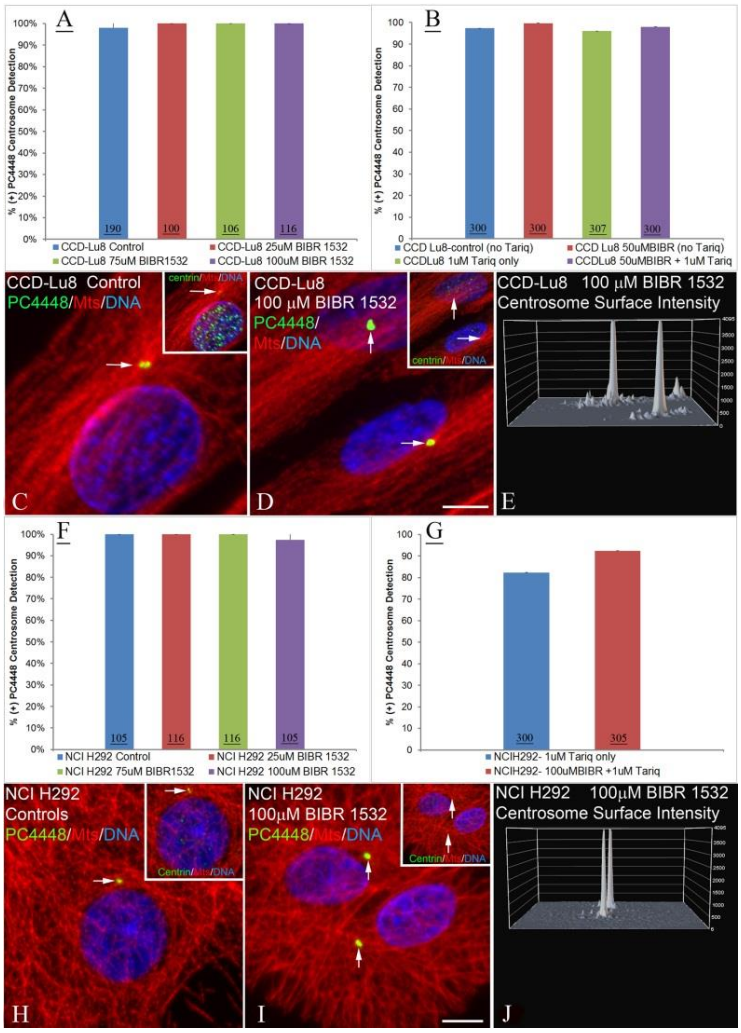

Figure 9. BIBR1532 effects on centrosome detection with pericentrin antibody 4448 (PC4448) in control CCD-Lu8 lung fibroblasts and NCI H292 cancer cells. A: CCD-Lu8 exposed to 0, 25µM, 75µM, or 100µM BIBR1532 for 6 days without tariquidar MDR inhibitor. Analysis of methanol-fixed cells expressing 1 or 2 centrosomes per cell as detected by pericentrin antibody PC4448 antibody was plotted against BIBR1532 exposure concentration. No impact on centrosome detection or amplification was observed. Numbers represent total cells scored. B: CCD-Lu8 cells exposed to 50µM BIBR1532 for 6 days, either with or without 1µM tariquidar MDR inhibitor, and compared to non-exposed TI cells either with or without tariquidar. No significant impact on centrosome detection or duplication was detected. Numbers represent total cells scored over three independent trials. C-E: GFP centrin- expressing control CCD-Lu8 lung cancer cells, without tariquidar, showing pericentriolar PC4448 (C: green, arrow), GFP centrin at centrioles (C: inset, arrow), and cytoplasmic microtubule detection (C: red; DNA, blue) in a typical interphase cell. GFP-centrin CCD-Lu8 cells treated with 100 µM BIBR1532 for 6 days did not alter detection of pericentrin PC4448 (D: green, arrows), although centrin detection had significantly reduced intensity (D: inset, arrows). E: PC4448 centrosome surface intensity profile of the GFP centrin–tagged cells imaged in panel D, showing no intensity differences in the microtubule organizing centers of adjacent cells. F: NCI H292 cells exposed to BIBR1532 without tariquidar as described for cells in panel A. We observed no changes in centrosome detection or normal centrosome numbers in the cytoplasm after 6-day treatment with BIBR1532. Numbers represent total cells scored. G: NCI H292 cells treated for 6 days with 100µM BIBR1532 and 1µM tariquidar compared to NCI H292 cells incubated with tariquidar alone. Although a small reduction in detecting 1-2 centrosomes per cell was observed overall, it was not statistically significant. H-J: image panels of GFP centrin-tagged NCI H292 cells stained for PC4448 (green, arrows), microtubules (red) and DNA (blue). No significant reduction in PC4448 detection at centrosomes was observed between control (H: green, arrow) and BIBR1532 treated cells (I: green, arrows), although GFP centrin detection was significantly reduced after BIBR1532 (I: inset, green, arrows). J: centrosome surface intensity profile in the pair of adjacent cells in panel, I showing no loss of PC4448 pericentrin after 6-day treatment with BIBR1532. All images are triple-labeled for pericentrin PC4448 (green), cy5 microtubules (red) and DNA (blue). Bars=5µm.

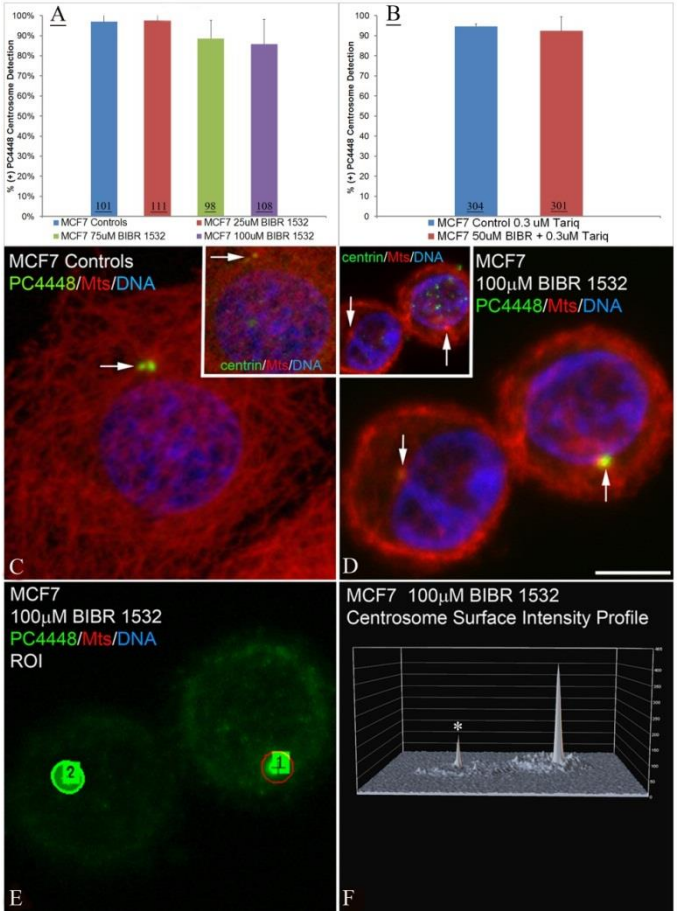

Figure 10. BIBR1532 effects on centrosome detection with pericentrin antibody 4448 (PC4448) in MCF7 breast adenocarcinoma cells. A: graphic representation of PC4448 pericentrin detection in MCF7 cells grown for 6 days in 0, 25µM, 75 µM, or 100µM BIBR1532 without tariquidar. A slight reduction in the percentage of cells with 1-2 centrosomes per cell was observed in TI concentrations ≥ 75µM, although these results were not statistically significant compared to non-drug-treated MCF7 cancer cells. Numbers represent total cells scored. B: centrosome detection in control (no TI) and 50µM BIBR1532 interphase MCF7 cells with 0.3µM tariquidar for 6 days, demonstrating no reduction in detection of 1-2 cytoplasmic centrosomes. Numbers represent total cells from three independent experiments. C: image of fixed, stained GFP centrin tagged control (no TI) MCF7 cells, showing centrosomes labeled with PC44486 (C: green, arrow), microtubules (C: red), and Hoechst DNA (blue) and expressing GFP centrin at the centrioles (C: inset, arrow). D: a minority of GFP centrin-tagged MCF7 cells cultured in the presence of 100 µM BIBR1532 for 6 days showed vastly reduced PC4448 staining at the centrosome (D: left cell, green, arrow; red, microtubules; blue, DNA). Note that the staining pattern of the GFP centrin was also reduced (D: inset, green, arrows). E: image depiction of two region of interests drawn around the cytoplasmic centrosomes and used to determine the surface intensity profile of PC4448 staining for the cells shown in panel D. F: significantly reduced centrosome surface intensity profile in left cell in panel E observed after culture in 100 µM BIBR1532 without tariquidar (* marks centrosomes with reduced surface intensity). All images are triple-labeled for pericentrin PC4448 (green), cy5 microtubules (red) and DNA (blue). Bars=5µm.

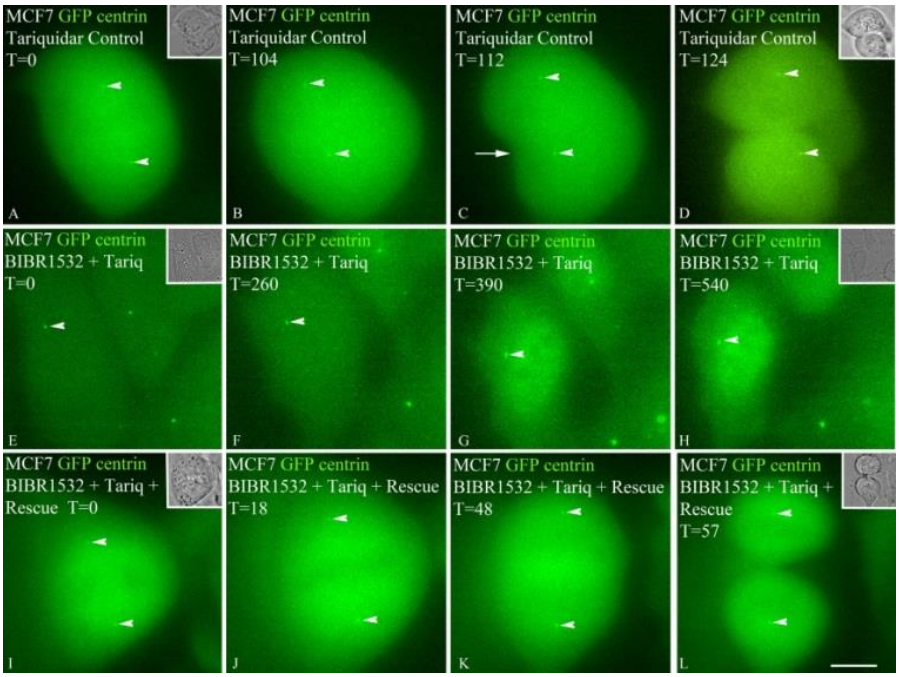

Figure 11. Time-lapse video microscopy of GFP centrin-tagged MCF7 cells in the presence of the telomerase inhibitor BIBR1532 for 48 hrs. A-D: GFP centrin MCF7 cells imaged in 1µM tariquidar multidrug resistance inhibitor, showing bipolar spindle assembly with centrioles at each spindle pole (arrowheads) and ultimate cell division within 2 hrs post-imaging (D: inset, brightfield). E-H: GFP centrin-tagged MCF7 cells imaged in the presence of 1µM tariquidar with 75µM BIBR1532 for 9 hrs. Although this cell appeared to round up and enter into mitosis, the centrosomes never duplicated or separated at the beginning of mitosis (G: arrowhead) and the cell failed to progress through mitosis or division (H: inset, bright field). I-L: GFP centrin MCF7 cells were treated with tariquidar + BIBR1532 for 48 hrs and allowed to recover for 48 hrs in normal culture medium before imaging. Note: a bipolar spindle is assembled with duplicated split centrioles (I: arrowheads), with normal cell division occurring by 57 min post imaging (L: inset, bright field). Image times are shown in each panel. Arrowheads depict GFP-tagged centrioles. Insets in A, E, and I are bright field optics pre-imaging, while insets in D, H, and L are bright field optics post-image acquisition. Bar= 5µm.

Table 1. Summary of spindle assembly checkpoint antibodies tested in control and cancer cell lines after exposure to BIBR1532 and/or tariquidar MDR inhibitor.

		Detection in CCD Lu8 Mitotic Cells		Detection in NCI H292 Mitotic Cells			Detection in MCF7 Mitotic Cells		
		Tariq only	Tariq + BIBR 1532	Ctr	Tariq only	Tariq + BIBR 1532	Ctr	Tariq only	Tariq + BIBR 1532
Probe (host)	Source								
Aurora A (rabbit)	Novus Biologicals	+++	+++	+++	+++	+	+++	+++	+++
Aurora B (rabbit)	Millipore Clone EP1009Y	ND	+	++	++	+	++	++	++
Bub1 (mouse)	Millipore Clone 14H5	ND	+++	+++	++	++	+	+	++
Mad1 (mouse)	Millipore Clone 9B10	-	ND	ND	-	-	ND	-	+
Anti-tubulin YOL134 (rat)	Millipore	+++	+++	+++	+++	+++	+++	+++	+++

Key: +++: strong detection; ++: moderate detection; +: weak detection; -: no detection; ND: not determined; Ctr: control, non-drug treated cells; Tariq: tariquidar inhibitor.

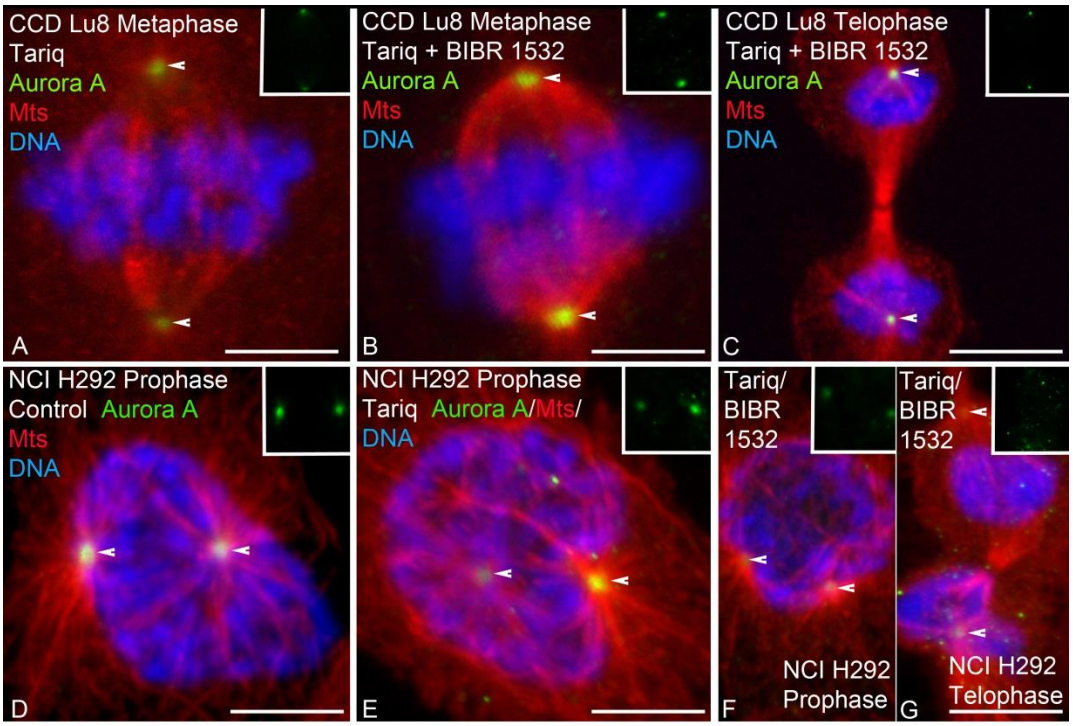

Figure 12. Detection of Aurora A in cancer cells after BIBR1532 and tariquidar MDR inhibitor exposure. A-C: Mitotic stage CCD-Lu8 control lung fibroblast cells. Aurora A antibody is detected at the centrosomes at metaphase (A-B; green, arrowheads; red, microtubules; blue, DNA) after exposure to 1µM tariquidar (A) or simultaneous treatment in 100µM BIBR1532 and 1µM tariquidar (B) for 48 hrs. At late telophase (C: red, microtubules, blue, DNA), Aurora A is also expressed at spindle pole centrosomes (C: green, arrowheads) after dual exposure to tariquidar/BIBR1532 for 48 hrs. Insets, A-C: details of centrosomal labeling with Aurora A. D-I: NCI H292 lung fibroblast cells. At prophase, Aurora A is strongly detected at the dual, split centrosomes (D: green, arrowheads) as microtubules assemble (D: red; blue, DNA) in both control (D) and 1µM tariquidar-treated cells (E) for 48 hr. However, prophase and telophase NCI-H292 cells that assemble in the presence of 1µM tariquidar and 100µM BIBR1532, after 48 hrs incubation, showed reduced Aurora A detection at the centrosomes (F and G: green, arrowheads), despite centrosomes separating, microtubule nucleation, and cell division (F: red, microtubules; blue, DNA). D-G, insets: details of centrosomal detection with Aurora A antibody). Bars=5µm.

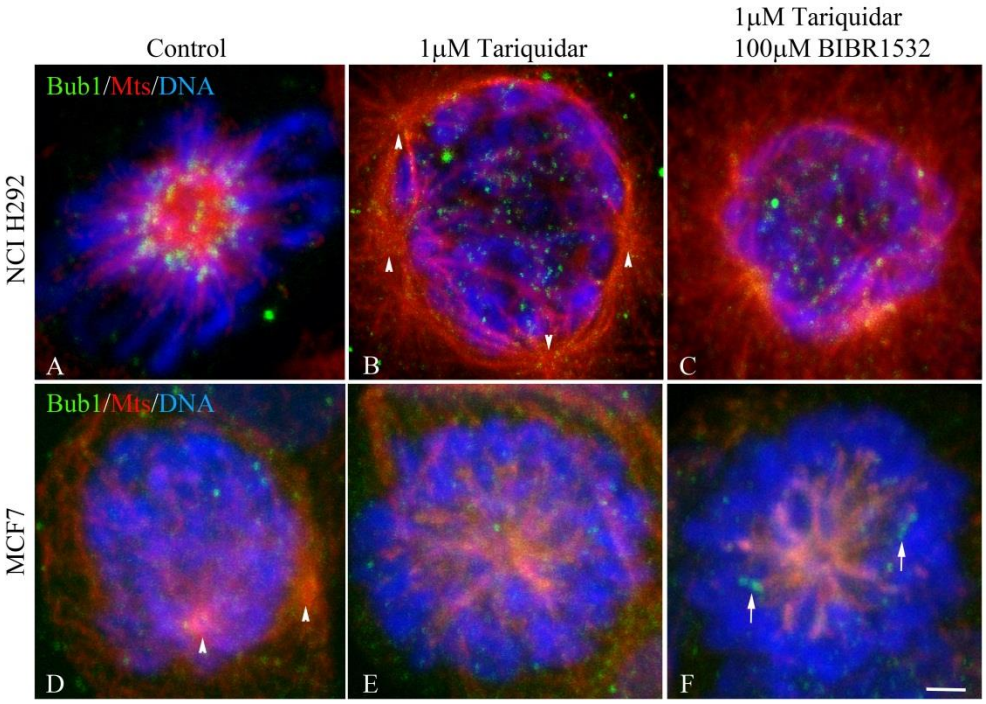

Figure 13. Detection of Bub1 in prophase NCI H292 and MCF7 cancer cells following BIBR1532 exposure. A-C: Bub1 antibody detection in NCI H292 control (A: green), 1μM tariquidar (B: green; arrowheads mark centrosomes) and simultaneous exposure to 1μM tariquidar with 100μM BIBR1532 (C: green; red, microtubules; blue, DNA). Bub1 is strongly detected in non-drug treated NCI H292 cells compared to cancer cells treated with tariquidar and/or BIBR1532. D-F. Bub1 antibody detection in MCF7 breast adenocarcinoma cells. Weak detection of Bub1 was found in control (D: green; arrowheads depict centrosomes) and 1μM tariquidar-exposed cells (E: green) compared to MCF7 cancer cells exposed simultaneously to 1μM tariquidar and BIBR1532 (F: green, arrows). All images are triple-labeled for Bub1 (green), microtubules (red), and DNA (blue). Bar=5μm.

References.

1. Brewster, A.M, Hortobagyi, GN, Broglio, KR, Kau, S-W, et al (2008). Residual Risk of Breast Cancer Recurrence 5 years After Adjuvant Therapy. J Natl Cancer Inst 100: 1179-1183.
2. Sugimura, H., Nichols, FC, Yang, P., Allen, MS, Cassivi, SD, et al (2007). Survival after recurrent nonsmall-cell lung cancer after complete pulmonary resection. Ann Thorac Surg 83: 409-418
3. O'Flaherty, JD, Barr, M, Fennell, D, Richard, D, Reynolds, J, et al (2012). The cancer stem cell hypothesis: Its emerging role in lung cancer biology and its relevance for future therapy. J Thorac Oncol 7:1880-1890.
4. Podberezin, M, Wen, J., and Chang, C-C (2012). Cancer stem cells: a review of potential clinical applications. Arch Pathol Lab Med [epub ahead of print] doi: 10.5858/arpa.2012-0494-RA.
5. Buseman, CM, Wright, WE, Shay, JW (2012). Is telomerase a viable target in cancer? Mutation Res 730:90-97.
6. Shay, JW and Wright, WE (2011). Role of telomeres and telomerase in cancer. Sem Cancer Biol 21:349-353.
7. Shay, JW, Reddel, RR, and Wright, WE (2012). Cancer and Telomeres- an ALTernative to telomerase. Science 336: 1388-1390.
8. Damm, K, Hemmann, U, Garin-Chesa, P., Hauel, N., Kauffmann, I, et al (2001). A highly selective telomerase inhibitor limiting human cancer cell proliferation. EMBO J 20: 6958-6968.
9. Bashash, D., Ghaffari, SH, Zaker, F., Hezave, K., Kazerani, M. et al (2012). Direct short-term cytotoxic effects of BIBR 1532 on acute promyelocytic leukemia cells through induction of p21 coupled with downregulation of c-myc and hTERT transcription. Cancer Inves 30: 57-64.
10. Pascolo, E, Wenz, C, Lingner, J, Hauel, N, Priepke, H et al (2002). Mechanism of human telomerase inhibition by BIBR 1532, a synethic, non-nucleosidic drug candidate. J Biol Chem 277: 15566-15572.
11. Dikmen, ZG, Gellert, GC, Jackson, S, Gryaznov, S, Tressler, R., et al (2005). In vivo inhibition of lung cancer by GRN163L: a novel human telomerase inhibitor. Cancer Res 65: 7866-7873.
12. Abraham, RT (2001). Cell cycle checkpoint signaling through ATM and ATR kinases Genes Dev 15:2177-2196.
13. Musacchio, A and Salmon, ED (2007). The spindle assembly checkpoint in space and time Nat Rev Mol Cell Biol 8:379-393.
14. Qi, W and Yu, H (2006) The spindle checkpoint and chromosome stability. Genome Dynamics 1:116-130.
15. Bharadwaj, R. and Yu, H. (2004) The spindle checkpoint, aneuploidy, and cancer. Oncogene 23: 2016-2027.
16. Kim, S, Sun, H, Tomchick, DR, Yu, H. and Luo, X. (2012) Structure of human Mad1 c-terminal domain reveals its involvement in kinetochore targeting. Pro Natl Acad Sci USA 109:6549-6554.
17. Katayama, H. and Sen S. (2010). Aurora kinase inhibitors as anticancer molecules. Biochem Biophys Acta 1799: 829-839.

18. Sasai, K, Katayama, H, Stenoien, DL, Fujii, S, Honda, R, Kimura, M, et al. (2004) Aurora-C kinase is a novel chromosomal passenger protein that can complement Aurora B kinase function in mitotic cells. Cell Motil Cytoskel 59:249-263.
19. Slattery SD, Mancini, MA, Brinkley, BR and Hall, RM. (2009). Aurora-C kinase supports mitotic progression in the absence of Aurora B. Cell cycle 8: 2984-2994.
20. Fry, Am, O'Regan, L, Sabir, SR, and Bayliss, R. (2012). Cell cycle regulation by the Nek family of protein kinases. J. Cell Sci. 125: 4423-4433.
21. Perpelescu, M and Fukagawa, T (2011). The ABCs of CENPs. Chromosoma 120:425-446.
22. Briasoulis, E, Kamposioras, K, Tzovaras, V, Pafitanis, G, Kostoula, A., Mavridis, A., and Pavlidis, N. (2008). CENP-B specific anti-centromere autoantibodies heralding small-cell lung cancer. A case study and review of the literature. Lung Can 60: 302-306.
23. Kleideiter, E, PIotrowska, K, and Klotz, U. (2008). Screening of telomerase inhibitors. In: Methods in Molecular Biology (ed LG Andrews, and TO Tollefsbol) 405: 167-180, Humana Press Inc. Totowa, NJ.
24. Simerly C, Schatten G. (1993). Techniques for localization of specific molecules in oocytes and embryos. Methods Enzymol 225:516-53.

18. Extent of Clinical Activities Initiated and Completed. Items 18(A) and 18(B) should be completed for all research projects. If the project was restricted to secondary analysis of clinical data or data analysis of clinical research, then responses to 18(A) and 18(B) should be "No."

18(A) Did you initiate a study that involved the testing of treatment, prevention or diagnostic procedures on human subjects?

_____Yes
___x__No

18(B) Did you complete a study that involved the testing of treatment, prevention or diagnostic procedures on human subjects?

_____Yes
__x___No

If "Yes" to either 18(A) or 18(B), items 18(C) – (F) must also be completed. (Do NOT complete 18(C-F) if 18(A) and 18(B) are both "No.")

18(C) How many hospital and health care professionals were involved in the research project?

_____Number of hospital and health care professionals involved in the research project

18(D) How many subjects were included in the study compared to targeted goals?

_____Number of subjects originally targeted to be included in the study
_____Number of subjects enrolled in the study

Note: Studies that fall dramatically short on recruitment are encouraged to provide the details of their recruitment efforts in Item 17, Progress in Achieving Research Goals, Objectives and Aims. For example, the number of eligible subjects approached, the number that refused to participate and the reasons for refusal. Without this information it is difficult to discern whether eligibility criteria were too restrictive or the study simply did not appeal to subjects.

18(E) How many subjects were enrolled in the study by gender, ethnicity and race?

Gender:
_____Males
_____Females
_____Unknown

Ethnicity:
_____Latinos or Hispanics
_____Not Latinos or Hispanics
_____Unknown

Race:
_____American Indian or Alaska Native
_____Asian
_____Blacks or African American
_____Native Hawaiian or Other Pacific Islander
_____White
_____Other, specify:_____
_____Unknown

18(F) Where was the research study conducted? (List the county where the research study was conducted. If the treatment, prevention and diagnostic tests were offered in more than one county, list all of the counties where the research study was conducted.)

19. Human Embryonic Stem Cell Research. Item 19(A) should be completed for all research projects. If the research project involved human embryonic stem cells, items 19(B) and 19(C) must also be completed.

19(A) Did this project involve, in any capacity, human embryonic stem cells?
_____Yes
__x___ No

19(B) Were these stem cell lines NIH-approved lines that were derived outside of Pennsylvania?
_____Yes

_____ No

19(C) Please describe how this project involved human embryonic stem cells:

20. Articles Submitted to Peer-Reviewed Publications.

20(A) Identify all publications that resulted from the research performed during the funding period and that have been submitted to peer-reviewed publications. Do not list journal abstracts or presentations at professional meetings; abstract and meeting presentations should be listed at the end of item 17. **Include only those publications that acknowledge the Pennsylvania Department of Health as a funding source** (as required in the grant agreement). List the title of the journal article, the authors, the name of the peer-reviewed publication, the month and year when it was submitted, and the status of publication (submitted for publication, accepted for publication or published.). Submit an electronic copy of each publication or paper submitted for publication, listed in the table, in a PDF version 5.0.5 (or greater) format, 1,200 dpi. Filenames for each publication should include the number of the research project, the last name of the PI, and an abbreviated title of the publication. For example, if you submit two publications for Smith (PI for Project 01), one publication for Zhang (PI for Project 03), and one publication for Bates (PI for Project 04), the filenames would be:

Project 01 – Smith – Three cases of isolated
Project 01 – Smith – Investigation of NEB1 deletions
Project 03 – Zhang – Molecular profiling of aromatase
Project 04 – Bates – Neonatal intensive care

If the publication is not available electronically, provide 5 paper copies of the publication.

Note: The grant agreement requires that recipients acknowledge the Pennsylvania Department of Health funding in all publications. Please ensure that all publications listed acknowledge the Department of Health funding. If a publication does not acknowledge the funding from the Commonwealth, do not list the publication.

Title of Journal Article:	Authors:	Name of Peer-reviewed Publication:	Month and Year Submitted:	Publication Status (check appropriate box below):
1. None				☐Submitted ☐Accepted ☐Published
2.				☐Submitted ☐Accepted ☐Published

20(B) Based on this project, are you planning to submit articles to peer-reviewed publications in the future?

Yes___x_____ No_____

If yes, please describe your plans:

The discoveries reported here are being analyzed and confirmed. Once that work is completed, then they will be prepared for publication in a prominent cell and cancer biology journal.

21. Changes in Outcome, Impact and Effectiveness Attributable to the Research Project.
Describe the outcome, impact, and effectiveness of the research project by summarizing its impact on the incidence of disease, death from disease, stage of disease at time of diagnosis, or other relevant measures of outcome, impact or effectiveness of the research project. If there were no changes, insert "None"; do not use "Not applicable." Responses must be single-spaced below, and no smaller than 12-point type. DO NOT DELETE THESE INSTRUCTIONS. There is no limit to the length of your response.
None.

22. Major Discoveries, New Drugs, and New Approaches for Prevention Diagnosis and Treatment. Describe major discoveries, new drugs, and new approaches for prevention, diagnosis and treatment that are attributable to the completed research project. If there were no major discoveries, drugs or approaches, insert "None"; do not use "Not applicable." Responses must be single-spaced below, and no smaller than 12-point type. DO NOT DELETE THESE INSTRUCTIONS. There is no limit to the length of your response.
None

23. Inventions, Patents and Commercial Development Opportunities.

23(A) Were any inventions, which may be patentable or otherwise protectable under Title 35 of the United States Code, conceived or first actually reduced to practice in the performance of work under this health research grant? Yes_____ No____x_____

If "Yes" to 23(A), complete items a – g below for each invention. (Do NOT complete items a - g if 23(A) is "No.")

a. Title of Invention:

b. Name of Inventor(s):

c. Technical Description of Invention (describe nature, purpose, operation and physical, chemical, biological or electrical characteristics of the invention):

d. Was a patent filed for the invention conceived or first actually reduced to practice in the performance of work under this health research grant?
Yes_____ No____

If yes, indicate date patent was filed:

e. Was a patent issued for the invention conceived or first actually reduced to practice in the performance of work under this health research grant?
Yes_____ No____
If yes, indicate number of patent, title and date issued:
Patent number:
Title of patent:
Date issued:

f. Were any licenses granted for the patent obtained as a result of work performed under this health research grant? Yes_____ No____

If yes, how many licenses were granted?_____

g. Were any commercial development activities taken to develop the invention into a commercial product or service for manufacture or sale? Yes___ No____

If yes, describe the commercial development activities:

23(B) Based on the results of this project, are you planning to file for any licenses or patents, or undertake any commercial development opportunities in the future?

Yes_____ No____x_____

If yes, please describe your plans:

24. Key Investigator Qualifications. Briefly describe the education, research interests and experience and professional commitments of the Principal Investigator and all other key investigators. In place of narrative you may insert the NIH biosketch form here; however, please limit each biosketch to 1-2 pages. *For Nonformula grants only – include information for only those key investigators whose biosketches were not included in the original grant application.*

BIOGRAPHICAL SKETCH

NAME	POSITION TITLE
Calvin Simerly, PhD	Research Associate Professor

INSTITUTION AND LOCATION	DEGREE *(if applicable)*	YEAR(s)	FIELD OF STUDY
Pensacola Junior College, Pensacola, Florida	A.A.	1974-1976	Biology
Florida State University Tallahassee, Florida	B.S.	1976-1979	Biological Science
University of Wisconsin Madison, Wisconsin	Ph.D.	1995-1998	Endocrinology-Reproductive Sciences

A. Positions and Honors Positions (since 1995)

1995-1997	Department of Zoology, University of Wisconsin, Madison, Wisconsin	Assistant Scientist
1997-1998	Division of Reproductive Sciences Oregon Regional Primate Research Center Beaverton, Oregon	Staff Scientist I
1997-1998	Division of Reproductive Sciences Oregon Regional Primate Research Center Beaverton, Oregon	Staff Scientist I
1998-2001	Division of Reproductive Sciences Oregon Regional Primate Research Center Beaverton, Oregonm	Staff Scientist II (Assistant Professor Equivalent)
1999-2001	Department of Obstetrics/Gynecology Oregon Health & Science University Portland, Oregon	Research Assistant Professor
2001-2008	Department of Obstetrics/Gynecology & Reproductive Sciences, University of Pittsburgh Pittsburgh, Pennsylvania	Associate Professor
2008-Present	Department of Obstetrics/Gynecology & Reproductive Sciences, University of Pittsburgh Pittsburgh, Pennsylvania	Research Associate Prof

B. Selected Perr-Reviewed Publications

1. Schatten G, Schatten H, **Simerly C**: Detection of sequestered calcium during mitosis in mammalian cell cultures and in mitotic apparatus isolated from sea urchin zygotes. Cell Biol Intl Rep, 6(8):717-724, 1982.
2. **Simerly C**, Wu G, Zoran S, Ord T, Rawlins R, Jones J, Navara C, Gerrity M, Rinehart J, Binor Z, Asch R, Schatten G: The paternal inheritance of the centrosome, the cell's microtubule-organizing center, in humans and the implications for infertility. Nat Medicine 1:47-53, 1995.
3. **Simerly C**, Zoran SS, Payne C, Dominko T, Sutovsky P, Navara CS, Salisbury JL, Schatten G: Biparental inheritance of γ-tubulin during human fertilization: Molecular reconstitution

of functional zygotic centrosomes in inseminated human oocytes and in cell-free extracts nucleated by human sperm. Mol Biol Cell 10(9):2955-2969, 1999.

4. **Simerly C**, McFarland D, Castro C, Lin CC, Redinger C, Jacoby E, Mich-Basso J, Orwig K, Mills P, Ahrens E, Navara C, Schatten G. Interspecies chimera between primate embryonic stem cells and mouse embryos: monkey ESCs engraft into mouse embryos, but not post-implantation fetuses. Stem Cell Res. 2011 Jul;7(1):28-40. doi: 10.1016/j.scr.2011.03.002. Epub 2011 Mar 25. PMID: 21543277.
5. **Simerly C**, Schatten G. Utility of animal models for human embryo culture: nonhuman primates. Methods Mol Biol. 2012;912:39-59. doi: 10.1007/978-1-61779-971-6_4. PMID: 22829368.
6. Easley CA 4th, Phillips BT, McGuire MM, Barringer JM, Valli H, Hermann BP, **Simerly CR**, Rajkovic A, Miki T, Orwig KE, Schatten GP. Direct differentiation of human pluripotent stem cells into haploid spermatogenic cells. Cell Rep. 2012 Sep 27;2(3):440-6. doi: 10.1016/j.celrep.2012.07.015. Epub 2012 Aug 23. PMID: 22921399.
7. Easley, CA. 4th, **Simerly, C.R**., Schatten, G. (2013). Stem cell therapeutic possibilities: future therapeutic options for male-factor and female-factor infertility? Reprod Biomed Online. Jul;27(1):75-80. doi: 10.1016/j.rbmo.2013.03.003. Epub 2013 Mar 26.
8. Easley, CA., Latov, DR., **Simerly, C.R**., Schatten, G. (2014). Adult Somatic Cells to the Rescue: Nuclear Reporgramming and the Dispensablity of Gonadal Germ Cells. Fert Steril 101:14-19

C. RESEARCH SUPPORT

1R25CA163168-01 (Schatten, G.)
Frontiers in Stem Cells in Cancer 9/26/11–8/31/16
NIH/NCI
This training course offers annual Cancer Education short-courses as well as limited support for subsequent pilot research projects and on-going mentoring.

1T15 HD072833 (Schatten, G.P.)
Rehabilitative and Regenerative Medicine for
Minority Health & Health Disparities 9/10/12 – 8/31/15
NIH/NICHD
The overall purpose of this NICHD Continuing Education Training Program is to provide comprehensive and sophisticated training and state-of-the-art methods on bioengineering, cellular, molecular and genetic approaches for advancing the Frontiers in Rehabilitative and Regenerative Medicine for rectifying Minority Health and Health Disparities.

R25 AG043365 (Schatten, G.P)
Frontiers in Aging and Regenerative Medicine 9/30/12-8/31/17
NIH/NIA
Frontiers in Aging and Regenerative Medicine (FrARR) trains and mentors promising junior and senior undergraduates from predominately underrepresented communities in sophisticated aging research and encourages and supports them as they embark on graduate studies.

BIOGRAPHICAL SKETCH			
NAME Schatten, Gerald P. PhD	POSITION TITLE Professor and Vice Chair of Obstetrics, Gynecology& Reproductive Sciences		
INSTITUTION AND LOCATION	DEGREE *(if applicable)*	YEAR(s)	FIELD OF STUDY
University of California, Berkeley	A.B.	1971	Zoology
University of California, Berkeley	Ph.D.	1975	Cell Biology
Rockefeller Foundation Fellowship	Postdoc	1976	Reprod Biology
German Cancer Research Center, Heidelberg	Postdoc	1976	Cancer Biology
Rockefeller Foundation Fellowship	Postdoc	1977	Reprod Biology

A. Position and Honors

Positions

1975 Instructor, Department of Zoology, Univ. of California, Berkeley.
1976, 1977 Rockefeller Foundation Postdoctoral Fellowship.
1977, 1984 Guest Researcher, German Cancer Research Center, Heidelberg.
1977-1986 Assistant (1977-81), Assoc (1981-85), Prof (1986), Molecular Biophysics; Florida State Univ.
1981-1986 Research Career Development Award, National Institutes of Health.
1985, 1986 Instructor in Embryology, Marine Biological Laboratory, Woods Hole.
1986-1997 Professor of Zoology, Molecular Biology & Ob/Gyn, University of Wisconsin
1986-1992 Director, Integrated Microscopy Resource, University of Wisconsin.
1987-1997 Director, Gamete & Embryo Biology NIH Training Program Core Scientist, Wisconsin Regional Primate Research Center
1997-2001 Endowed Professor of OB/GYN and Cell/Developmental Biology, Oregon Health Sciences University; and Senior Scientist, Oregon Regional Primate Research Center
1998-2001 Founding Course Director, "Frontiers in Reproduction," MBL, Woods Hole
1997-2008 NIH MERIT Award
2001-Pres. Director, Pittsburgh Development Center,Professor and Vice Chair, Ob/Gyn and Reproductive Sciences, Professor of Cell Biology- Physiology, & of Bioengineering, University of Pittsburgh School of Medicine

B. Selected Peer-reviewed Publications (Selected from > 270 peer-reviewed publications)

1. Huleihel L, Ben-Yehudah A, Milosevic J, Yu G, Pandit K, Sakamoto K, Yousef H, Lejeune M, Coon TA, Redinger CJ, Chensny L, Manor E, Schatten G, Kaminski N. let-7d microRNA affects mesenchymal phenotypic properties of lung fibroblasts. Am J Physiol Lung Cell Mol Physiol. 2014 Jan 17. [Epub ahead of print] PubMed PMID: 24441869.
2. Easley CA 4th, Latov DR, Simerly CR, Schatten G. Adult somatic cells to the rescue: nuclear reprogramming and the dispensability of gonadal germ cells. Fertil Steril. 2014 Jan;101(1):14-9. doi: 10.1016/j.fertnstert.2013.11.025. Review. PubMed PMID: 24382340.
3. Easley CA 4th, Simerly CR, Schatten G. Stem cell therapeutic possibilities: future therapeutic options for male-factor and female-factor infertility? Reprod Biomed Online.

2013 Jul;27(1):75-80. doi: 10.1016/j.rbmo.2013.03.003. Epub 2013 Mar 26. Review. PubMed PMID: 23664220; PubMed Central PMCID: PMC3703485.
4. Shi Q, Schatten G, Hodara V, Simerly C, VandeBerg JL. Endothelial reconstitution by CD34+ progenitors derived from baboon embryonic stem cells. J Cell Mol Med. 2013 Feb;17(2):242-51. doi: 10.1111/jcmm.12002. Epub 2013 Jan 10. PubMed PMID: 23301772; PubMed Central PMCID: PMC3814022.
5. Cibelli J, Emborg ME, Prockop DJ, Roberts M, Schatten G, Rao M, Harding J, Mirochnitchenko O. Strategies for improving animal models for regenerative medicine. Cell Stem Cell. 2013 Mar 7;12(3):271-4. doi: 10.1016/j.stem.2013.01.004. PubMed PMID: 23472868.

C. Research Support

1 U13 HD061150 (Schatten, G. 0% funding)Frontiers in Stem Cells and Regeneration
5/1/09-4/30/14 NIH/NICHD
This training course provides comprehensive training in methods and state-of-the art technology for pluripotent stem and germ cell research and regenerative medicine.

5 R01 MH087247-02 (Ayyavoo, V.) HIV-1 Associated Dementia: Concomitant Roles of Vpr and Cellular Factors
3/9/10–2/28/15NIH/NIMH
The goal is to understand the factors involved in HIV-1 induced neurodegeneration.

1 R01 HL102177 (Carlisle, D.)Nicotine Dysregulates Lung Differentiation through N-myc
4/1/11 – 3/31/16NIH/NHLBI
This proposal will provide a mechanism for the decreased lung function seen in infants born to smoking mothers, and be used to guide the development of new interventions to improve the lung health of infants and children.

1R25CA163168-01 (Schatten, G.) Frontiers in Stem Cells in Cancer
9/26/11–8/31/16 NIH/NCI
This training course offers annual Cancer Education short-courses as well as limited support for subsequent pilot research projects and on-going mentoring.

1T15 HD072833 (Schatten, G.P.) Rehabilitative and Regenerative Medicine for Minority Health & Health Disparities
9/10/12 – 8/31/15 NIH/NICHD
The overall purpose of this NICHD Continuing Education Training Program is to provide comprehensive and sophisticated training and state-of-the-art methods on bioengineering, cellular, molecular and genetic approaches for advancing the Frontiers in Rehabilitative and Regenerative Medicine for rectifying Minority Health and Health Disparities.

R25 AG043365 (Schatten, G.P) Frontiers in Aging and Regenerative Reseach
9/30/12-5/31/17 NIH/NIA
Frontiers in Aging and Regenerative Medicine (FrARR) trains and mentors promising junior and senior undergraduates from predominately underrepresented communities in sophisticated aging research and encourages and supports them as they embark on graduate studies.